N71-20333
NASA CR-72826
S-71-1017

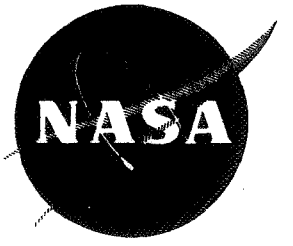

SPIRAL GROOVE FACE SEAL DEVELOPMENT FOR SNAP 8

by

A. J. Orsino
J. A. Findlay

Dr. H. J. Sneck
(Retained Consultant - Rensselaer Polytechnic Institute - Troy, N. Y.)

prepared for

NATIONAL AERONAUTICS AND SPACE ADMINISTRATION

NASA LEWIS RESEARCH CENTER

Contract NAS 3-11824

Andre J. Stromquist, Project Manager

GENERAL ELECTRIC COMPANY
CORPORATE RESEARCH AND DEVELOPMENT
Schenectady, N.Y.

GENERAL ELECTRIC

Requests for copies of this report should be referred to

National Aeronautics and Space Administration
Office of Scientific and Technical Information
Attention: AFSS-A
Washington, D.C. 20546

NASA CR-72826
S-71-1017

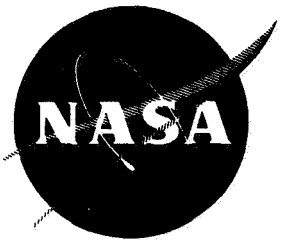

SPIRAL GROOVE FACE SEAL DEVELOPMENT FOR SNAP 8

by

A. J. Orsino
J. A. Findlay

Dr. H. J. Sneck
(Retained Consultant - Rensselaer Polytechnic Institute - Troy, N. Y.)

prepared for

NATIONAL AERONAUTICS AND SPACE ADMINISTRATION

NASA LEWIS RESEARCH CENTER

Contract NAS 3-11824

Andre J. Stromquist, Project Manager

GENERAL ELECTRIC COMPANY
CORPORATE RESEARCH AND DEVELOPMENT
Schenectady, N.Y.

GENERAL ELECTRIC

NASA CR-72826
S-71-1017

FINAL REPORT

SPIRAL GROOVE FACE SEAL DEVELOPMENT

FOR

SNAP-8

by

A. J. Orsino
J. A. Findlay
Dr. H. J. Sneck (Retained Consultant)

Prepared for

NATIONAL AERONAUTICS AND SPACE ADMINISTRATION

AUGUST 7, 1970

CONTRACT NAS 3-11824

NASA LEWIS RESEARCH CENTER
CLEVELAND, OHIO
ANDRE J. STROMQUIST, PROJECT MANAGER
POWER CONVERSION SYSTEMS

GENERAL ELECTRIC COMPANY
Corporate Research and Development
Schenectady, New York

TABLE OF CONTENTS

TABLE OF CONTENTS

FOREWORD

The work described herein, which was conducted by the General Electric Company, Research and Development Center, was performed under NASA Contract NAS 3-11824. The work was done under the management of NASA Project Manager, Mr. Andre J. Stromquist, Power Conversion Systems Section, NASA-Lewis Research Center. The work was performed from May 31, 1968 to August 7, 1970.

SPIRAL GROOVE FACE SEAL DEVELOPMENT FOR SNAP 8

by

A.J. Orsino, J.A. Findlay

Dr. H.J. Sneck

(Retained Consultant - Rensselaer Polytechnic Institute - Troy, N.Y.)

ABSTRACT

This report presents detailed information regarding the design and test of a spiral groove face seal for use on the SNAP-8 alternator as a self-actuated shut-down seal. The concept is intended to improve system reliability by assuring the presence of lubricant in the bearing cavity at all times. The experimental work which was carried out in the initial phase of the project on a bronze seal, indicated that the concept would be an attractive adjunct to the SNAP-8 system and would not compromise the performance of current prototype seals. Experiments, performed during the last phase of the project, were carried out using a seal made from tool steel. The purpose was to demonstrate that a seal, which was compatible with the SNAP-8 system, could successfully complete a 2500 hour endurance run and 100 start-stops. The seal failed at the beginning of these tests. The cause of this failure was most likely either a foreign particle in the seal, or seal warpage.

I. INTRODUCTION AND SUMMARY

SNAP-8 is a light weight nuclear powered electrical generating system for space application. The three phase 400 cycle alternator, rated at 35 KW, is driven by a mercury vapor turbine. The alternator operates on conventional precision ball bearings which are lubricated with polyphenyl ether which also serves as a coolant. To meet high system reliability requirements the alternator is equipped with dynamic seals which prevent flow of lubricant into the alternator cavity during operation. These seals have performed in a satisfactory manner serving the dual functions of seals as well as bearing cavity lubricant scavengers.

Operational tests have indicated a need for assuring the presence of lubrication in the bearing cavity at time of system startup. Lubricant can be supplied to the bearing prior to startup but some adequate sealing means must be available to prevent excessive amounts of oil from entering the alternator cavity while still maintaining high system reliability. The spiral groove concept, as described in LeRCTND-3942,* provides at once a zero speed sealing effectiveness while simultaneously possessing a means for development of a significant hydrodynamic fluid film at the sealing interface under dynamic conditions. The fluid film serves to prevent the metal to metal contact which gives rise to wear, limited life and low reliability as found in conventional contact type face seals frequently referred to as mechanical seals. At transitional speeds, prior to development of a full fluid film, some metal to metal sliding contact may be present.

This contract effort was devoted to the implementation of the spiral groove concept into a simulated SNAP-8 alternator test assembly. More specifically, the work involved the analysis, design, fabrication and evaluation of a spiral groove shutdown seal that could be incorporated into the envelope of the present alternator without compromising the operation of existing seals.

The simulated SNAP-8 alternator test assembly had been used for development of the dynamic seals currently in use. The shutdown seal was designed in cooperation with personnel of NASA Lewis Research Center and was incorporated at the outboard anti-drive end of the test unit. A bellows arrangement was used to support the nosepiece which was mated directly to the outboard slinger.

* Also "Spiral Groove Face Seal Concepts; Comparison to Conventional Face Contact Seals in Sealing Liquid Sodium (400 to 1000°F)", T. N. Strom, L. P. Ludwig, G. P. Allen, R. L. Johnson, Lewis Research Center, NASA, Cleveland, Ohio, ASME 67-WA/LUB 17.

Testing, on the bronze seal, included static leakage evaluations taken periodically during the test program as well as a 50 hour continuous test at rated speed. In addition, 100 start-stop cycles executed in groups of ten cycles each followed by leakage evaluation at zero speed were performed. Lift off evaluation data as determined by capacitance probes mounted on the seal flange were obtained in order to formulate some correlation with design criteria.

Results of the testing during this phase were considered satisfactory. No evidence of distress at the seal interface was detected during any of the testing or subsequent visual inspections. Dynamic leakage during the fifty hour test was not measurable. Static leakage under high differential pressure was greater than expected, but for low differentials, as is the case under operational conditions, the flow was acceptably low.

Bronze is not a compatible material for the SNAP-8 system. Therefore, tests using a seal made from tool steel were initiated in order to demonstrate the operability and material compatibility of the face seal, over a long term endurance period; and during start-stop operation. The choice of material, and manufacturing procedure were established in cooperation with NASA personnel. The SNAP-8 test assembly was modified for unattended operation.

Results of this testing were negative. The seal was severely damaged during the first attempt to run it. The deep scratches in the seal and slinger appear to have been caused by a foreign particle entering the seal clearance. The seal was then refinished to a shallower groove depth and run again. The seal surface was almost completely destroyed during this test. The results indicate that there was insufficient lift-off and possible seal warpage.

This report presents design details of the seal arrangement as well as results of the various tests and the associated evaluation.

II. SEAL DESIGN AND PERFORMANCE ANALYSIS

A. Mechanical Design

1. Demonstration of Design Principle Tests (Bronze Seal)

Design of the shutdown seal was based on use of the spiral groove concept frequently used in thrust bearing applications for incompressible as well as compressible fluids. Extension of this principle to a face seal is outlined in NASA LeRC TN D-3942 for a liquid sodium system. For seal applications, the

the spiral interface may contain appropriate "dams" or the spiral may be of a "herringbone" pattern. For this work the dam and spiral arrangement was used.

A fundamental requirement for successful operation of the spiral groove seal is the need to provide a sufficient amount of lubricant to maintain the fluid film which is continuously being pumped by the groove pattern. Two different designs were considered for providing a continuous supply of lubricant to the interface namely the re-circulating arrangement and the positive feed arrangement. In both arrangements the nosepiece is supported by a metal bellows and is mated to the outboard slinger. The re-circulating design, Figure 1, provides a series of re-circulation passages which allow oil to flow to the center of the spiral groove pattern. In dynamic operation, oil in the spiral grooves becomes pressurized and is pumped back into the oil cavity. The slinger output controls oil cavity pressure. In the positive feed design, Figure 2, the re-circulation passage in the nosepiece is eliminated. However, the outboard slinger is modified to provide a pumping action for oil which can be subsequently supplied to the center of the spiral groove pattern. A portion of the oil injected onto the slinger by the oil ring is retained in the slinger dam prior to its entry into the "pump" passage. At rated speed a pressure in excess of 15 lb/in^2 could be generated in the slinger passages providing an adequate oil supply is maintained in the slinger dam.

The spiral groove pattern would be identical for either design and is shown in plane view, along with its associated dams, in Figure 3. The equation used for the coordinates shown were obtained from the following equation:

$$r = r_1 e^{\theta \tan\alpha}$$

where

r = radius coordinate of spiral

r_1 = inside radius of spiral pattern

θ = angular coordinate of spiral

α = spiral angle

The re-circulating arrangement was selected for detail design. Figure 4 is a detail drawing of the nosepiece showing the center distribution groove as well as the interconnecting passages.

Bellows selection was based on spring rate and mean effective diameter. To facilitate procurement, a standard bellows with a mean effective diameter

equal to 2.176 inch was purchased. The bellows spring rate was approximately 40 lb/in.. Some variations in mean effective diameter as well as spring rate were found in the bellows assembly obtained, however these were not considered critical to the test. The mean effective diameter is significant only at static sealing conditions and consequently did not effect the dynamic portion of the testing. The spring rate was somewhat lower than desired but this did not cause any problem since it was possible to provide additional deflection to obtain the desired loading. The stainless steel bellows are of an all metal welded construction.

Two seal nosepieces were manufactured of SAE 660 bronze to facilitate manufacture. It was recognized that this material would not be acceptable for final SNAP-8 prototype application. Two different techniques were employed to develop the sprial groove pattern; namely, chemical etching and end milling. The etching did provide a sharper pattern, although some undercutting was evident. Etching of harder materials such as M-50 bearing steel is possible in the annealled or hardened condition although machining of the center distribution channel and the interconnecting passageways would be best accomplished in the soft condition.

An extended view of the bellows assembly, the nosepiece and the slinger is shown in Figure 5. The bellows housing is shown with three oil exit ports. Although not evident in the photograph, the slinger mating face was coated with 0.003 inches of flame plated tungsten carbide.

2. Demonstration of Material Compatibility Tests (Steel Seal)

The bearing bronze material SAE 660 used for the hydrodynamic testing is considered to be adequate for meeting the life requirements in an oil environment, but not adequate for meeting requirements in the presence of mercury. Based on this knowledge, a change in nosepiece material is necessary to allow use of this type of shutdown seal in the SNAP-8 system. To assure increased resistance to wear, under conditions of boundary lubrication, a material capable of providing a relatively high hardness is desired. Increased hardness promotes increased difficulty of fabrication since groove depth as well as flatness must be maintained to fairly close tolerances. Although machining techniques are available for use on high hardness materials, their application to complex fabrications is frequently of a developmental nature, prone to unpredictable results and time consuming. A preferred approach would be to accomplish as much of the

machining as possible, employing conventional techniques before heat treatment to obtain the desired hardness. Unfortunately, it is extremely difficult to control distortions which may appear after heat treatment.

The use of low distortion die steels was considered since it was felt that they might allow complete fabrication prior to heat treatment without excess distortion. Some minor distortions could be permitted providing a final grinding and lapping of the seal surface would remove the distortion without compromising groove depth or otherwise adversely affecting the seal surfaces.

A favorable material might be found in one of the bearing steels, such as vacuum melt 52100 or M50, or in a 400 series hardenable stainless steel. It was recommended that solid tungsten carbide not be considered because of cost and the cycle time might be long. Flame plating of tungsten carbide was not recommended since the techniques for masking the details of the seal appeared to be rather undefined. A vendor contacted for flame plating on an inquiry basis could not offer any encouraging approach.

Both chemical etching and EDM were considered as techniques to aid in the manufacture of the seal. Both of these techniques are subject to certain unknowns which may produce unexpected difficulties. It was decided against using either of these techniques because of the expense and the masking problem. Whereas these methods may be used for forming the spiral groove pattern, there are oil feed holes and a deep circumferential groove that must also be put in. It was difficult to determine a sequence for accomplishing these steps in the manufacture of the seal that was satisfactory.

It was decided to select a material that would allow the seal to be made entirely by mechanical machining. The material choice was narrowed down to two; AISI A2 air hardened die steel (1% carbon, 5% chrome) and 17-4 PH stainless steel. A test blank was made from each material and heat treated. Measurements taken before and after the heat treatment indicated distortions of .0002" or less. In consultation with NASA metallurgists, and with the agreement of the SNAP-8 prime contractor, the die steel was chosen as the seal material. The heat treatment sequence decided upon for the spiral grooved seal was as follows:

a) Rough machine the seal

b) Soften at 1600°F

c) Machine all over leaving .002", mill in grooves .004" deep (.002" oversize) using the Masterline Tracer, machine in the circumferential groove, and drill the oil holes.

d) Harden by;
heating slowly to 1300-1400°F,
equilibrate,
heat faster to 1750-1800°F,
air quench,
temper twice at 700°F (RC57).

e) Final machine (grind) except face,
leave .002" on face.

f) Temper once at 700°F,
temper a second time at 600°F.

g) Final machine (grind) face and lap.

When the final grinding and lapping was started, the seal was found to have a warp of .0006" to .0008". This is compared to .0002" or less measured in tests prior to fabrication. In addition there was some variation in the depth of the grooves. The seal was ground and lapped flat to within .000020" and the final groove depths were as follows:

.0018	.0020	.0024	.0020
.0017	.0020	.0022	.0024
.0018	.0020	.0020	.0024
.0019	.0020	.0023	.0025
.0020	.0020	.0020	.0029
.0022	.0021	.0019	.0028
.0020	.0021	.0020	.0029
.0017	.0021	.0020	.0028
.0018	.0018	.0021	.0028

B. Analysis

1. Introduction

The analysis used will incorporate that employed by Muijderman* in his book on spiral groove thrust bearings. This analysis was developed for spiral groove thrust bearings which typically have larger radial spans than face seals. The theory developed by Muijderman is approximate in the sense that it does not satisfy the boundary conditions at the inner and outer radii. Corrections are made to the theory which are supposed to make up for this deficiency. For thrust bearings these corrections are small, but when applied to narrow radial-span face seals they can be quite large. For this reason, the predictions based on the theory which appears below can only be considered

*E. A. Muijderman, Spiral Groove Bearings, Springer-Verlag, New York, 1966.

as rough estimates whose precision is uncertain. Figure 6 is a radial cross-sectional view of the spiral groove face seal geometry used for this analysis.

2. Back-up Region

The back-up distance as predicted by the simple theory taken from Muijderman is given by

$$d_o = \frac{(P_2 - P_1)\, h_2^2}{6\eta\, U_2\, g_1}$$

where g_1 is a geometric factor of the form

$$g_1 = \frac{\gamma H^2 \cot\alpha\, (1 - H)\, (1 - H^3)}{(1+\gamma H^3)\, (\gamma + H^3) + H^3\, (\cot\alpha)^2\, (1+\gamma)^2}$$

When corrected for end-effects this distance is

$$d_1 = d_o + a_1\, (1 - \frac{\alpha}{90})\, \tan \left(\frac{1 - H^3}{1 + H^3}\right) \left[\frac{A_1 \cot\alpha}{A_1 \cot\alpha + C_1}\right]$$

Since the back-up region is a non-flow region, no leakage calculations are performed on it. The distance d_1 is important in that it must not exceed the distance $R_2 - R_1$ if leakage to the inside of the seal is to be prevented.

The separating force due to the pressure in this region is calculated from

$$F_1 = 2P_2\pi\, d_1 R_2 - \frac{3\pi\eta\, \omega R_2^4}{2h_2^2} \left[\frac{2d_o}{R_2}\right]^2 g_1$$

3. Region Between Seal Inner Radius and Fluid Interface

In this region the internal hydrostatic pressure acts on the seal surface so that

$$F_o = (P_o = P_1)\, \pi \left[(R_2 - d_1)^2 - R_o^2\right]$$

4. Feeding Groove Region

As with the previous region, the pressure is uniform over the region, so that

$$F_4 = 2\, \pi\, R_2 P_2 D$$

Spiral Groove Pumping Region

This region is similar to the back-up region with the exception that the pumping effects the pressure distribution and hence the separating force. This force is computed from the formula

$$F_2 = P_3\pi \left[R_3^2 - (R_2 + D)^2\right] - \frac{3\pi\eta\omega R_3^4}{2h_2^2} \left[\frac{2d}{R_3}\right]^2 g_1$$

$$- \left(\frac{12\eta S_t g_2}{\rho h_1 h_2^2}\right) \left[\frac{R_3^2 - (R_2+D)^2}{4}\right.$$

$$\left. - \frac{(R_2+D)^2}{2} \ln\left(\frac{R_3}{R_2+D}\right)\right] (1+\gamma)$$

where

$$g_2 = \frac{H^2 (1 + \cot^2\alpha)(\gamma + H^3)}{(1+\gamma H^3)(\gamma + H^3) + H^3 (\cot\alpha)^2 (1+\gamma)^2}$$

and S_t is the through-flow pumping rate.

5. Outer Dam Region

In this region the separating force is given by*

$$F_3 = \pi P_3 (R_4^2 - R_3^2) + \frac{2\pi (P_3 - P_4)}{\ln (R_4/R_3)} \left[\frac{R_4^2 - R_3^2}{4}\right.$$

$$\left. - \frac{R_4^2}{2} \ln \frac{R_4}{R_3}\right]$$

6. Flow Rate Matching

The flow-rate across the spiral groove portion of the seal must equal the flow-rate across the outer dam. Both of these flow-rates are controlled by the pressure P_3. If P_3 is eliminated from the flow-rate equations for these regions, the mass flow-rate from R_2 to R_4 is given by

*Equation (30) of "Effects of Geometry and Inertia on Face Seal performance - Laminar Flow", Jr. of Lub. Tech., Vol. 90, Series F, No. 2, April '68, p. 333.

$$S_t = \left[\frac{g_1 + \dfrac{(P_2 - P_4)\, h_2^2}{6\eta\, U_3 d}}{\dfrac{\ln (R_4/R_3)}{\pi d U_3 \rho\, h_2} + \dfrac{2g_2}{U_3 h_1 a_1 \rho\, k}} \right]$$

In this equation the distance d is not the radial span of the spiral groove pumping section. It is that distance corrected for the end effects at both the inner and outer radii, and is computed from

$$d = d_2 - a_1 \left(1 - \frac{\alpha}{90}\right) \tan \alpha \left(\frac{1 - H^3}{1 + H^3}\right)$$

7. Computational Procedure

If the seal geometry, fluid properties and P_1, P_2, and P_4 are known, then d, d_1, and S_t can be computed directly. The pressure P_3 can then be computed from

$$P_3 = P_4 + \frac{6\eta\, S_t \ln (R_4/R_3)}{\pi \rho\, h_2^3}$$

and the total force found from

$$F = F_o + F_1 + F_2 + F_3 + F_4$$

A computer program was set up to facilitate the numerical computation of the above quantities. A listing of this program in time-sharing FORTRAN language is given in Appendix A.

As a back-up to the force calculations, a simplified calculation was also made assuming that there were straight line pressure distributions between the pressures P_1, P_2, P_3, and P_4. With this assumed trapizoidal distribution, an approximate separation force (W) was computed and printed out for comparison with the presumably more accurate value F. This force was always lower than F, indicating that the simplified linear pressure distribution assumption yields conservative estimates of the separating force generated by the seal. Intuitively, this is what was expected.

8. Nomenclature (For Seal Analysis)

a_1 = Tangential width of the groove

a_2 = Tangential width of the ridge

A_1 = Pressure distribution constant (See Muijderman)

C_1 = Pressure distribution constant (See Muijderman)

d = Distance d_2 corrected for end effects

D = Width of circumferential feeding groove

d_o = Uncorrected radial length of the back-up region

d_1 = Radial length of fluid back-up region

d_2 = Radial length of spiral groove pumping region

F = Total separating force

F_o = Separating force exerted by internally applied pressure $P_o = P_1$

F_1 = Separating force exerted by pressure in back-up region d_1

F_2 = Separating force exerted by pressure in spiral groove pumping region d_2

F_3 = Separating force exerted by pressure in the outer dam region

F_4 = Separating force exerted by pressure P_2 in circumferential feeding groove

g_1 = Geometry factor for pressure drop

g_2 = Geometry factor for pressure force

h_o = Groove depth

$h_1 = h_o + h_2$

h_2 = Dam clearance = minimum clearance

$H = h_2/h_1$

k = Number of grooves

P_o = Internally applied pressure

$P_1 = P_o$

P_2 = Supply pressure at feeding groove

P_3 = Pressure at step entrance to dam

P_4 = Externally applied pressure

S_t = Mass flow-rate leakage through seal

U_2 = Tangential velocity at R_2 ; ($U_2 = R_2\omega$)

U_3 = Tangential velocity at R_3 ; ($U_3 = R_3\omega$)

α = Spiral groove angle

$\gamma = a_2/a_1$

η = Viscosity

ρ = Density

ω = Rotational angular velocity

III. TEST APPARATUS

A. Introduction

The experimental work was performed on the SNAP-8 test equipment previously fabricated under NAS 5-417 in conjunction with development of non-contracting dynamic seals for the SNAP-8 alternator. The apparatus is capable of simulating the alternator operating conditions to an extent considered sufficient for testing of the alternator bearing and seal system. No provision is made to simulate weightlessness as associated with a zero-gravity environment. Pressures, temperatures, speed, and oil flow are readily controlled. Principal radial and axial dimensions are similar to the prototype alternator. To facilitate the testing, the spiral groove shutdown seal was incorporated into the outboard anti-drive end of the test apparatus.

B. Description of Test Unit

The test assembly consists of the following major elements mounted on a slotted base plate:

Rotor and Casing Assembly
Thymotrol Drive Assembly
Lubricant System Assembly

Figure 7 shows the unmodified alternator test assembly with the arrangement of bearings and seals as tested under NAS 5-417. The modification incorporated in

the outboard anti-drive end for the work described in this report is shown in Figure 8. The outboard screw seal was removed and the necessary changes made to incorporate the spiral groove seal and bellows assembly. A photograph of the test apparatus is shown in Figure 9. The electronic console and oscillograph were used in conjunction with the capacitance probes during lift evaluation testing.

The rotor is mounted on 208 angular contact bearings which are preloaded by two sets of wavy springs. The quill drive was used to allow torque measurement in the previous test program. The 250 watt calrod heating elements which surround the rotor are used to simulate pole face losses.

Surrounding the casing is an outer shroud used to simulate the stator cooling passages used in the prototype alternator. At the drive end two conventional carbon face seals are used.

Four plastic collection traps were provided to monitor leakage from the seals. For the testing described in this report, only leakage at the outboard anti-drive end was monitored for record since this was the location of the seal under test.

Vacuum conditions were maintained in the system with mechanical oil-sealed rotary sumps. The sump pressure was held at approximately 5 psia with a Welch Model 1405 pump (33.4 leters/min at 10^{-3} mm) and the stator cavity was held at approximately 29 inches Hg vacuum by a Welch Model 1402 (76 leters/min at 1 mm Hg).

The "thymatrol" drive assembly features a 7 1/2 HP direct current motor with a wide range speed of 13,200 rpm. The dynamic breaking feature was not used due to the limited torque range of the quill. The flexible quill was sized to allow a determination of stead-state input torque. Precision collets were used to connect the quill to the main rotor and to the drive spindle.

A schematic of the lubrication system is shown in Figure 10. The seven gallon cylindrical oil sump contains a 2 KW calrod heater with automatic temperature control. Oil is circulated by 3 GPM gear pump (Sunstrand Model BPD-052-200). Sump pressure could be maintained without audible evidence of cavitation. A heat exchanger was connected to the pump discharge and was used to provide further control of lubricant inlet temperature. A 10 micron glass element filter was used in the bearing feed lines to assure a clean oil supply. The

lubrication system was connected to the rotor and casing assembly by flexible braided hoses.

C. Description of Instrumentation

Identification and location of the instrumentation used during test can be made by reference to Figure 10 and Figure 11. The instrumentation is essentially identical to that used on previous SNAP-8 tests although several additions were made to satisfy requirements of the current testing. For example a differential pressure gauge was installed across the spiral groove seal to provide a direct reading. For the lift evaluation testing, capacitance probes (number 24 in Figure 11) were installed.

Pressure measurements were made with Bourdon tube gauges having an accuracy of 1/2% of full scale. Bearing inlet oil pressure was measured on a 0 to 60 psig gauge whereas bearing cavity, oil sump, bearing outlet oil, and alternator cavity pressures were measured on -30 to +30 psi compound pressure gauges. The differential pressure across the seal was measured on a 0 to 25 psi gauge.

Bearing temperatures were taken with spring loaded temperature probes located directly against the outer races. Three equally spaced probes were used. Standard bare wire copper-constantan thermocouples were used at other locations and their output was continuously recorded on a Leeds and Northrup temperature recorder. A mercury in glass thermometer showed oil sump temperature.

The speed signal was generated by a magnetic pickup which sensed three pins located on the spindle pulley. A digital display of speed was provided by a standard Hewlet Packard electronic counter.

Seal oil film thickness was measured by means of capacitive type transducers made for use with Wayne-Kerr DM100B distance meters. Data was taken by photographing the meter outputs as displayed on an oscilloscope. The output sensitivity was 250 microinches per centimeter. The transducers have a linear output over a range of .002 inches. Figure 12 shows an unmounted transducer with its integral coaxial lead. Three transducers were mounted to the bellows seal assembly as shown in Figure 13 for lift off evaluation. The probes were positioned .001 below the surface of the seal interface.

Leakage was collected at the plastic traps. Since the temperature of these traps was essentially room temperature and substantially below the temperature

of oil circulating in the test rig they did tend to act as cold traps. Although a cold trap at lower temperature would have had a greater pumping efficiency, calculations showed that any additional lubricant vapor loss from the system would be negligible.

The traps are made of 6.25 cm diameter plastic tube with a capacity of 3.07 cc per mm of tube height. The smallest unit of height measurement discernible was 0.25 mm. This gave a sensitivity of 0.766 cc.

In order to accomplish the endurance evaluation (2500 hours) at a minimum cost, it was necessary to modify the SNAP-8 test assembly to allow prolonged unattended operation. The unit was equipped with various monitoring devices capable of providing adequate safety for the equipment during its operation. The following additions were made to the system:

a) Speed Monitor - The system is shut down for either high speed (12,500 rpm) or low speed (9,500 rpm). At low speed the seal may not lift off far enough and result in excessive seal wear and possible failure.

b) Draintank and Heater - A drain tank is necessary to allow sufficient capacity for malfunction shutdown.

c) Oil Pump Timer - If the system is shut down, it is necessary to maintain lubricating oil flow until the rotor coasts down. The oil pump timer is activated when power to the test unit is shut off.

d) Vibration Motor - If the vibration of the test unit exceeds its normal operating level, then the unit is shut down automatically. This assumes that the excess vibrations was caused by some malfunction or failure.

e) Temperature Monitors - If the oil temperatures rise above $320^{\circ}F$, power to the test unit is automatically shut off.

f) Oil Level Monitor - If the oil level in the oil supply tank falls below the minimum set point, the unit is stopped.

g) Oil Pump Pressure Monitor - The power is shut off if the system pressure falls below 15.5 psi.

h) Cavity Pressure Monitor - The set point is 18" Hg vacuum for the cavity pressure and 14" Hg for the tank.

i) Light Indicator Board - If the test unit is shut down by one of the monitoring systems, then a light on the indicator board will turn on to show what set point caused the trouble.

Pressure transducers were added to the system to supply the electrical signals necessary for the pressure monitors.

IV. TEST PROCEDURE

A. Demonstration of Design Principle Tests (Bronze Seal)

1. Introduction

Prior to testing, all calibrations were checked and completed. As in the previous tests, the temperature readings were continuously recorded. All other readings were manually recorded at selected periodic intervals, in general at each half hour. To facilitate maintenance of the correct pressure profile across the spiral groove, a precision differential gauge was installed. Although leakage was monitored at all trap locations, data was recorded at the outboard anti-drive location only since this was the location of the spiral groove seal being tested.

2. Standard Start Up and Test Procedure

The following procedure was generally used for all tests during this program:

1. Sump oil heaters were turned on and sump oil temperature raised to 200°F.

2. Oil system circulating pump was turned on and oil flow was established to casing outer jacket and carbon face seal assembly.

3. The vacuum system was turned on and the system was evacuated.

4. When the desired vacuum conditions were attained, the drive was slowly activated.

5. Oil was admitted to bearings and speed was increased to design conditions.

6. The necessary final adjustments to attain the nominal conditions for test were then executed.

7. Data were recorded every half hour of test or at otherwise acceptable time interval.

8. Shutdown was attained by power cutoff to drive unit and a free coast-down to zero speed. Oil flow was reduced manually, but maintained to assure adequate oil to bearings.

B. Demonstration of Material Compatibility Tests (Steel Seal)

The test procedure used for this part of the program was essentially the same as before. It was necessary, however, to deactivate the monitoring system during start-up. Once steady-state conditions had been reached, then the monitoring system was activated.

Static leakage tests were made before the unit was started up and after it was shut down.

V. TEST RESULTS

A. Introduction

To accomplish the intended program objectives, the testing work was separated into the following categories:

B. Zero Speed Leakage Testing (Bronze Seal)
C. Design Speed Preliminary Testing (Bronze Seal)
D. Fifty Hour Continuous Test (Bronze Seal)
E. Start-Stop Testing (Bronze Seal)
F. Lift-Off Evaluation (Bronze Seal)
G. Seal Lift Off Correlation (Bronze Seal)
H. Groove Depth Experiments (Bronze Seal)
I. Material Compatibility Tests (Steel Seal)

All dynamic testing was based on the following nominal operating conditions:

Sump Pressure	5 PSIA
Oil Inlet Temperature	210°F
Slinger Pressure Rise	7.5 PSI

Spiral Groove Seal	10.0 PSID
Speed	12000 RPM
Oil Flow	0.32 GPM (per brg.)

B. Zero Speed Leakage Testing

Following bench tests to assure the basic integrity of the spiral groove seal assembly, a series of static leakage tests (zero shaft speed) were performed. For these tests the shutoff valves to Traps 2, 3, and 4 were closed and the alternator cavity was filled with oil sufficient to assure an oil level above the bearing housing. The alternator cavity was then pressurized and leakage was monitored at Trap #1. Testing with oil at room temperature was performed at 5, 10, 15, and 20 PSIG with a hold time of one hour at each pressure. No leakage was observed.

The test was then repeated with oil at 158°F, as determined by bearing contact thermocouples, and with the alternator cavity at a pressure of 20 PSIG. Over a one hour test time some wetting was seen, but no measurable quantity could be accumulated. These tests showed that the initial static leakage, even for relatively high pressure differentials, was very acceptable. This information served as a basis for subsequent static leakage tests which were performed periodically to determine sealing effectiveness.

C. Design Speed Preliminary Testing (Tests 3 through 14)

Immediately following static leakage testing, a number of tests at vacuum and at atmospheric pressure were conducted to evaluate dynamic sealing effectiveness as well as to insure the overall integrity of the test equipment. A total test time in excess of 65 hours at nominal design conditions was accumulated. Some leakage was noted during the initial portion of this testing. However, it was attributed to an incorrectly installed oil ring which was detected at disassembly following Test #8. Subsequent testing, Test #10, for a total time of 6 1/2 hours at a pressure differential of approximately 12 PSI did not produce any measurable leakage. Short durations to 15 PSID were also investigated with the same result. Additional test data at rated conditions will be presented separately and as part of the 50 hour continuous test.

Test #11 of this series was actually a static test at zero speed. It was intended to provide information regarding the static sealing effectiveness of the spiral groove seal following more than fifty hours of rated conditions.

For this test, the alternator cavity was flooded and leakage was monitored at Trap #1. A summary of the results is as follows:

TEST #11

STATIC LEAKAGE DATA

Pres. Dif. PSI	Test Time Hrs.	Temp. (Brg.) °F	Leakage cc/hr
0	5	111[2]	0.0[3]
1.0	3	182	0.2
5.0	3	176[1]	10.0
10.0	0.5	182	20.0
20.0	0.5	182	32.0

1 - Start at 140°F

2 - Start at 188°F

3 - Not measurable

The data shows that static leakage was considerably greater during Test #11 than it was prior to dynamic testing. Although no distress of the mating surfaces could be seen apparently some deterioration of the surfaces did take place. This is not entirely conclusive since subsequent static testing, following significantly more time at rated speed, provided much lower leakage rates. This will be reviewed in connection with the start-stop testing. In any event, once the hydraulic design has been selected, a more favorable material combination can be obtained. It is quite possible that at very low speed metal to metal contact of sufficient magnitude may give rise to incidental surface markings which will promote static leakage. Although a filter was used in the lubrication system the presence of small dirt particles is possible. These might not affect a hard surface during dynamic operation but might easily mark the bronze interface used on these tests.

Upon completion of the static test, additional testing at design conditions (Tests 12, 13, and 14) were performed to further establish the leakage performance of the spiral groove shutdown seal. An additional 13 hours was accumulated while at rated conditions with no evidence of measurable leakage.

D. Fifty (50) Hour Continuous Test (Test #15)

In order to obtain an extended time leakage evaluation of the spiral groove design at nominal operating conditions, a 50 hour continuous test was

performed. This was essentially a "hands off" test in which leakage at dynamic conditions was continuously monitored at Trap #1. Slight changes in test conditions were due to major power changes associated with plant work schedules. For example, normal plant shutdown at the end of the first shift gave rise to a speed increase whereas the start of first shift operation produced a slight speed decrease. These swings were normally corrected by the automatic feature of the speed control.

The test data is shown in Table D-1 and is reproduced in its entirety as representative of the data taken during all dynamic testing on this program.

No change in the oil level at Trap #1 was detected during the entire test. The test was pleasingly uneventful with little change in the value of various readings. Although data was taken at each half hour interval for the first twelves hours of test, the data was recorded only at hour intervals thereafter.

The seal was disassembled for inspection and photographed for record purposes. Evidence of running did exist at the bronze nosepiece interface. However, there was no evidence of surface distress.

E. Start-Stop Testing (Test #16 through 26)

A total in excess of 100 start-stop tests, exclusive of those associated with other dynamic tests were performed. Testing was performed under vacuum in groups of ten start-stop cycles. After each ten such cycles, a one hour static leakage check was made at a differential pressure of 10 PSI.

Since the testing was done at vacuum, a considerable amount of oil was collected at Traps 2, 3, and 4. This occurred since at reduced speed the slinger seals are no longer capable of pumping lubricant back to the sump, and there is still a need to maintain oil at the bearing. The coastdown time is approximately five minutes since no braking is present. In a typical test of ten start-stop cycles approximately two gallons of lubricant were collected from Traps 2, 3, and 4. Interestingly, no additional oil was collected at Trap #1 during the dynamic testing.

During these tests, only a minimal amount of data were recorded. The tests were executed from zero speed with a rapid rise to 12000 RPM and a coastdown back to zero speed. Vacuum was maintained in the system. Oil inlet temperature as well as bearing outer race temperature were continuously monitored.

Speed data from these tests are a matter of record but will not in themselves appear to be a matter of significant interest. The static leakage data obtained at the conclusion of each cycles of ten cycle test is as follows:

START-STOP LEAKAGE DATA
(10 PSID)

Test #	Leakage* cc/hr
17	12
18	24
19	10
20	46
21	50
22	14
23	4
24	0
25	6
26	6

*Oil temperature approximately 200°F

The variation in static leakage was not entirely rationalized although there was some evidence to indicate that it was related to the technique used for flooding the alternator cavity in preparation for static rest. Flooding was accomplished by admitting oil through the bearing oil ring. This assured that only filtered oil would enter the bearing cavity. Rapid flooding, accomplished by raising bearing cavity pressures, usually lead to more static leakage. By way of comparison, it is noted that the comparable static leakage after Test #11 was 20 cc/hr at a temperature of 176°F and lower. This would indicate that although some anomalous leakage behavior was present, there was no gross change in sealing effectiveness between Test #11 and Test #26. Moreover, for pressure differentials of the order of the static oil head present in the alternator cavity no measurable oil leakage was detected during Test #25.

F. Lift-Off Evaluation

Lift speed characteristics were evaluated by means of the capacitance probes installed on the bellows assembly. Figure 13 shows the probes as installed for this series of tests. The data is important for two very specific reasons. That is, the speed at which initial lift can be detected is considered of great

interest. In addition, test data which would allow comparison of actual versus predicted lift is significant since it could form the basis for seal performance correlations.

Figure 14 is representative of the lift characteristic noted during tests started with bearing outer race temperature at 140°F. Lift is noted immediately after start and rises to a value of approximately .0008 inch at 1,000 rpm. As speed increases and as slinger pressure increases, there is a reduction of lift to the steady value of approximately 450 microinches. The actual curve is influenced by rate of speed increase as well as the inlet oil temperature and flow. For starts made with a high bearing outer race temperature the initial lift is somewhat lower. The difference is due to the greatly reduced oil viscosity resulting from the increase in oil temperature.

Data was also obtained from the comparison of actual seal lifts with the seal lift predicted from the rather simplified analysis presented in Section II of this report. Figure 15 shows the results obtained from the three capacitance probes at speeds of 12,000, 10,000 and 8,000 rpm. The results are plotted as a function of differential pressure across the spiral groove seal. The probe data indicates that the seal lift is not symmetrical. At a differential pressure of 10 psi, Probe 3 indicates an average lift of 370 microinches whereas Probe 1 shows an average lift of 490 microinches. An additional variation in probe data can be seen in Figure 16. The small amplitude is undoubtedly due to waviness or lack of squareness between the slinger and the shaft. Absolute values of lift are somewhat difficult to determine without an extensive survey of all the possible influences which might alter probe readings. Consequently, the values from Figure 15 should be considered to be somewhat approximate in nature.

It was possible to obtain data at a groove depth of 0.004 inch. This is represented in Figure 17 for a speed of 12,000 rpm. It can be seen that the lift characteristic is somewhat different from the data taken with the seal having the 0.002 inch groove depth. The data indicates that above a differential of 8.5 psi the film thickness is quite low. A review of this data and its correlations with the analysis used will be present in a subsequent section of this report.

G. Seal Lift-Off Correlation

Two seals were tested, one with a groove depth h_o = 0.002 inches and one with a groove depth h_o = 0.004 inches. Their dimensions were otherwise the same. These dimensions and other pertinent data are given below:

$R_o = 1.068"$ $\quad P_1 = 0$

$R_1 = 1.118"$ $\quad P_0 = 0$

$R_2 = 1.203"$ $\quad a_1 = 0.164"$

$R_3 = 1.288"$ $\quad a_2 = 0.060"$

$R_4 = 1.318"$ $\quad \omega = 1255$ radians/sec.

$k = 36$ $\quad \rho = 0.0397\ lb_m/in^3$

$D = 0.025"$

$d_2 = 0.060"$ $\quad \eta = 0.637\ (10^{-6})\ \frac{lb_f sec}{in^2}$

(ET378 at 240^oF)

The best results for these two seals are shown in Figures 15 and 17. The data selected from these curves (Probe 2) for processing through the mathematical model is given in the following tables:

$h_o = 0.002$ inches

$P_2 = P_4$ (PSI)	h_2 (Inches)
6	0.000512
8	0.000475
10	0.000436
12	0.000400
14	0.000360

$h_o = 0.004$ inches

$P_2 = P_4$ (PSI)	h_2 (Inches)
3	0.000540
4	0.000462
5	0.000385
6	0.000310
7	0.000235

It was not possible to measure through-flow in the test rig, but it was possible to measure the clearance h_2. The loading on the seal by the cavity pressure and bellows can be calculated from the formula

$$F = 8.0 + 1.66\ \Delta P$$

where F = load in lb_f

ΔP = seal pressure differential in PSI

The results of this calculation are shown in Figure 18. Also plotted on this same figure are the results of the computations using the proposed seal theory.

It was pointed out earlier that the end-corrections of Muijderman's theory were of doubtful accuracy where applied to seals which have R_1/R_2 approaching unity. For this reason, two different computations were made for each of the seals:

1. One calculation applies an end correction to both ends of the through-flow part of the spiral groove section (i.e., at $R_2 + D$ and R_3 using the formula given above for d).

2. The other calculation applies only one end correction at $R_2 + D$.

Figure 18 shows that the end correction has a strong effect on the magnitude of the hydrodynamically generated seal separating force. A glance at the curves will show that individual end corrections could be selected for each of the two seals which would yield excellent correlation between the theoretical model and experiment. This would amount to using an empirical "fractional" end correction. Figure 18 indicates that two different "fractional" end corrections for the $h_o = 0.002"$ and $h_o = 0.004"$ seals would probably be needed to bring test results into agreement with the applied loading. Unfortunately, there is no way of knowing what "fractional" end correction might be required for some other value of h_o. Difficulties of this sort were anticipated when the model was first proposed.

Another way of checking the model experimentally is to change the rotational speed of the seal. The test results of Figure 15 for $h_o = 0.002$ indicate that speed has little or no effect on h_2 as the speed is increased from 8,000 rpm to 12,000 rpm. Calculated response based on the theory does not show such

insensivity at all. Once again the theory could be "bent" to agree with the test data, but to do so would require the end-correction to be a function of ω. Intuitively this is not unreasonable, but the present theory does allow for this kind of dependence.

Having cited the theory's deficiencies, a few words should be said in its favor. It does yield lifting forces of the right order of magnitude. The predicted trend with changes in sealed pressure is correct and even accurate if the right "fractional" end-correction is used. The model predicted no leakage at operating speed and none was observed. The model predicted that the seal would lift-off and operate hydrodynamically and it did. The predicted through-flow pumping rate, although not verified with experimental data, is believable. At the design operating conditions of $P_2 = P_4 = 10$ psi with $h_o = 0.002$ and 12,000 rpm, the predicted through-flow pumping (two end corrections) is about 11.0 lbm/hr.

The table below shows the back-up distance d_1 for $h_o = 0.002$" rpm as computed using two end-corrections.

($h_o = 0.002$", 12,000 rpm)

$P_2 = P_4$ (PSI)	d_1 (Inches)
6	0.0503
8	0.0512
10	0.0514
12	0.0526
14	0.0530

This distance is only a little more than one-half the distance available before the fluid would reach the inner sealing land.

Based on the limited experimental evidence available, it appears that the proposed mathematical model for the seal as a whole has merit. In its present form, however, it is not a predictive model due primarily to poor theoretical model for the spiral groove portion of the seal.

There are two ways this problem could be rectified. One approach would be to attempt to fix-up the end-correction terms in Muijderman's analysis. The

experiments show that these corrections can be quite influential which is certainly not what is expected of a "correction". Without the end corrections this theory is not even close to the observed performance, so that the whole weight of correlation really rests on the end-corrections. One must conclude that if real accuracy depends on the correction terms Muijderman's analysis will require substantial modification before it becomes productive.

The other approach is to seek a new solution to the spiral groove portion which satisfies the end conditions exactly and does not require any end-corrections at all. Such a solution should be specifically constructed to solve the problems at hand, i.e., a narrow land seal.

To draw an analogy, Muijderman's thrust bearing analysis is comparable to Sommerfeld long journal bearing solution. Sommerfeld's solution is accurate only when the "ends" represent a small portion of the bearing length. What is really needed is a solution comparable to the short journal bearing solution of Ocvirk and DuBois where most of the bearing is "ends".

H. Groove Depth Experiments

This group of tests was conducted to obtain experimental data regarding the effect of spiral groove depth on seal lift, or interface separation, at 12,000 rpm. One nosepiece, which was successively ground to give shallower depths, was used for all experiments in order to limit manufacturing cost. The nosepiece was initially made with an average groove depth of 0.004 inches. The average depth was determined from measurements taken at twelve of the thirty-six grooves. Two depth values were taken for each groove at locations as shown on Figure 19. Table 2 gives the actual measured values from which the average depth was determined. The nosepiece, which was made of SAE 660 bearing bronze, was photoetched to produce the required spiral pattern prior to drilling of the feed holes.

In addition to the nosepiece used for these tests, one other nosepiece was made. For this nosepiece, the spiral grooves pattern was produced by end-milling. The average groove depth is 0.002 inches as determined by measurements taken at twelve of the thirty-six grooves. Table 3 gives the actual measured values which were taken in accordance with the method shown in Figure 19.

A study of the values shown in Tables H-1 and H-2 indicates a considerable degree of variation in the groove depth measurements. This is primarily due

TABLE H-1

SPIRAL GROOVE DEPTH MEASUREMENTS

ETCHED PATTERN

Groove Location	ID Depth Inches	OD Depth Inches
1	0.0037	0.0035
2	0.0042	0.0038
3	0.0043	0.0040
4	0.0043	0.0046
5	0.0040	0.0043
6	0.0037	0.0041
7	0.0030	0.0037
8	0.0035	0.0033
9	0.0041	0.0035
10	0.0050	0.0040
11	0.0050	0.0045
12	0.0046	0.0042

NOTE: Only 12 equally spaced grooves were measured.

TABLE H-2

SPIRAL GROOVE DEPTH MEASUREMENTS

MILLED PATTERN

Groove Location	ID Depth Inches	OD Depth Inches
1	0.0020	0.0020
2	0.0017	0.0020
3	0.0020	0.0022
4	0.0024	0.0025
5	0.0020	0.0021
6	0.0014	0.0015
7	0.0012	0.0007
8	0.0020	0.0012
9	0.0027	0.0024
10	0.0023	0.0017
11	0.0018	0.0015
12	0.0022	0.0022

NOTE: Only 12 equally spaced grooves were measured.

to the rather rough surface finish which exists at the bottom of each groove for "etched" as well as the "milled" nosepiece.

To supplement the initial data taken at 0.004 inches, tests were conducted at average groove depths of 0.003, 0.002 and 0.0015 inches.

As for most testing, the capacitance probes did not produce identical absolute lift measurements. Consequently, to facilitate presentation of the results from the groove depth experiments, the readings taken with probe #3 are shown. All data is for 12,000 rpm since no significant speed effect was detected. Figure 20 shows the data for the three tests and the data from Probe #3 in Figure 17. It can be seen that reduction of groove depth produces increase seal lift up to some unknown maximum lift after which it begins to drop rather significantly. Time did not permit an accurate determination of the groove depth which would produce maximum lift. Maximum lift was noted at 0.002 inches for the groove depths tested.

I. Material Compatibility Tests (Steel Seal)

The test rig was modified for unattended operation before the bronze seal was removed. Checkout runs were made to see if the monitoring system worked properly. These tests were performed while the steel seal was being manufactured and, therefore, the bronze seal was still in place. With some adjustments the monitoring system was determined to be in working order.

When the steel seal was completed the test unit was disassembled and the bronze seal removed. Inspection of the parts, at this time, revealed some minor wearing of the tungsten carbide plated slinger, which acts as the seal runner. The plated surface was ground and lapped flat and smooth. Before assembly of the new seal and refinished slinger, the oil system was drained and recharged with new oil (provided by NASA). The parts were carefully cleaned and the unit reassembled.

After the new spiral grooved face seal was installed, a static pressure test was made. Excessive leakage was measured over a range of pressures. In order to determine if the leakage was coming from the primary seal or from one of the secondary seals (O-rings), the test rig was brought up to speed and a dynamic leakage check made. Under dynamic operating conditions the pumping action of the spiral grooves should prevent any leakage through the primary seal. Excessive leakage did occur during this test, however, thus leading to

the conclusion that the secondary seals were most likely at fault. During this test, which lasted for about 30 minutes, the seal film thickness was measured and found to be approximately .000500 in.

The test unit was then disassembled and both the seal and slinger were found to be damaged. The nature of the damage indicated that a foreign particle had come between the mating surfaces of the seal. Several deep scratches were found in the runner and in the inside diameter dam and lands of the seal. The outside diameter dam and lands of the spiral grooved seal were undamaged. The runner showed some pickup of material. There was a very small nick out of one of the seal lands. This might have been the source of the damaging particle.

Both the seal and the slinger (runner) were repaired. This left the seal spiral grooves shallower than desired since about .0005 in. had to be removed from the seal surface. It was felt, however, that the seal should still be operable since previous tests had been made with .0015 in. deep grooves. Under these conditions the bronze seal had lifted off but ran with a reduced film thickness (.000260 in. at ΔP = 10 psi).

New O-rings were put in the assembly and the seal installed once again in the test unit. Static leakage tests indicated a reduced leak rate of 7 cc/hr. The previous excessive leakage might, therefore, have been due to the O-rings. The test unit was then brought up to speed in order to check the dynamic leakage. There was no detectable dynamic leakage. This seemed to confirm our conclusion that the previous leak had been stopped and the seal system was ready for testing. The seal was allowed, therefore, to run for a period of about 22 hours during which time the test set up and monitoring system was checked out again. Everything seemed to be in order for starting the endurance test with the exception of the film thickness probes. During this checkout run the signal from these probes was lost. This was not felt to be unusual, however, since it had occurred before and was due to oil coming between the probe and the measuring surface. Even though the film thickness measurements were not needed for carrying out the experiments, it was decided to disassemble the system before starting the extended endurance run and check it once more.

When the test unit was disassembled the seal and slinger were examined and found to be damaged. The damage was extensive showing evidence of the surface wiping for a rubbing type of wear was present. The wear affected the entire

seal surface, and to the extent that several of the grooves were completely obliterated. In addition to extensive wearing of the slinger (runner) surface, there was material pick-up on it and several deep scratches had penetrated the tungsten carbide flame plate. Indications were, however, that the tungsten carbide plating had been intact before the test began.

The important question at this point was; what had caused the seal failure, and how could it be corrected? The initial seal damage, resulting in the deep scratches, certainly must have been the most critical since it resulted in compromising the groove depth when the seal was repaired. It is not evident from that incident that there was any material incompatibility. The problem appeared to be caused by a single foreign particle, although this cannot be completely substantiated. Once the groove depth was reduced, the operating film thickness was also reduced, thus increasing the sensitivity of the seal to warpage. Examination of the damaged seal after the final test run, Figure 21, gives some indication of warpage. This may have been due to thermal conditions because of the greater heat generation in the thin film and the lower thermal conductivity of the steel seal compared to the bronze seal. The recorded temperatures did not show any marked rise during the test, however.

Further work on the program was terminated due to the negative results obtained.

VI. CONCLUSIONS

A. Demonstration of Design Principle Tests (Bronze Seal)

The work of this contract was devoted to the design and test of a spiral groove face seal for use as a self-actuated shutdown seal on SNAP 8 alternators. Such a seal would be intended to assure the presence of lubricant in the bearing cavity under startup and also under shutdown conditions. It is expected that this would provide an improvement in overall system reliability. The work involved extended duration steady-state testing as well as transient testing. Leakage was evaluated under various modes of operation.

Based on the data obtained during this program, the following conclusion may be drawn. The validity of these conclusions must be tempered by the knowledge that the actual test times were extremely short when compared to desired prototype life and reliability:

1. Integration of the spiral groove seal with the slinger seal has been shown to be a feasible design concept. The scavanging capability of

the slinger seal appeared to be in no way affected by the presence of the spiral groove seal which was mated directly to one face of the slinger seal on the outboard anti-drive end.

2. The spiral groove seal performed effectively as a substitute for the screw seal which was removed from the outboard anti-drive end during the tests. At nominal operating conditions, with a pressure differential of 10 psi across the spiral seal, the leakage would be acceptable in terms of SNAP 8 prototype requirements. This conclusion is based specifically on the results of the 50 hours continuous test during which no measurable leakage was accumulated.

3. Start-stop operation of the type performed during test should not be detrimental to seal life. No evidence of change in seal interface was detected as a result of the start-stop cycling during this test program.

4. Absolute magnitude of seal lift is influenced by temperature as predicted from the analysis. This provides a somewhat increased seal clearance under cold start conditions (with $150^{o}F$ bearing race temperature) but does not compromise the sealing effectiveness.

5. The configuration of spiral groove face seal tested during this program can be incorporated in the prototype unit on an interchangeable basis. This conclusion is based on the assumption that the SNAP 8 Alternator Test Assembly is adequately representative of the prototype units. To the best of all knowledge available such is indeed the case.

6. Static sealing at low differential pressures, of the order of static head contained in the bearing cavity, is expected to be acceptably low. This should be especially true for low temperatures.

7. It appears that a predictive analysis for performance of the spiral groove face seal is possible. Preliminary estimates of seal lift can be made based on available state-of-the-art knowledge. However, the corrections for end effects within the seal geometry greatly effect the absolute accuracy with which performance predictions can be made.

B. Demonstration of Material Compatibility Tests (Steel Seal)

This phase of the program was aimed at demonstrating the operability and material compatibility of the spiral groove face seal over a long term endurance period (2500 hours), and during 100 start-stop cycles. A material, A2 tool steel, was chosen that would be compatible with the SNAP-8 system. The bronze seal did not satisfy this condition.

The results of this phase of the program were inconclusive. This was due to the early failure of the seal. The first failure was apparently caused by a particle, of unknown origin, lodged between the seal surfaces. This particle may have been the small piece broken off the seal groove edge. This failure may have been due to material incompatibility, but the evidence is not strong enough to conclude this. Grinding off this damage left the seal with shallower grooves and, therefore, a reduced operating film thickness. This had the effect of increasing the seals sensativity to warpage. Therefore, insufficient lift-off and thermal warpage could have caused the second seal failure.

Subsequent to this seal failure, several General Electric materials engineers were consulted in regards to the seal material. Their recommendations were that if the A2 tool steel is used, it should be cooled to a low temperature for a period of from 24 to 48 hours, after the final heat treatment has been completed. If this is not done the retained austenite will cause the seal to distort.

It is felt that the spiral groove seal design principle has been adequately demonstrated. It remains to demonstrate material compatibility with a material that is satisfactory to use in the SNAP-8 system. The A2 tool steel may be satisfactory if some changes in the manufacturing procedure are made. However, before proceeding with the program, other materials should also be considered. Candidate materials might include solid tungsten carbide and solid carbon graphite.

VII. RECOMMENDATIONS

The overall analytical model proposed for the seal as a whole appears to be a reasonable description of the seal hydrodynamics. The weakest part of the model is obviously the part that describes the hydrodynamics of the spiral groove portion. Unfortunately, this is the most important part.

The Muijderman theory might be improved empirically by determining end corrections from test data. Considering the number of parameters involved this could be quite costly.

The other alternative is to develop an analysis which from the outset is designed to solve the specific problem at hand, namely the narrow land seal. As part of a separate activity, a preliminary investigation has been carried out which indicates that this can be done using the "narrow land" approximation which has proved successful in analyzing other seal configurations. This particular analytical approach not only satisfies the boundary conditions exactly, but it also can incorporate the contributions of fluid inertia which at higher speeds can have detrimental effect on seal performance.

It is expected that the analysis would be straight forward, but probably quite laborious, especially if a large number of geometric configurations are to be evaluated. The results would be expected to produce predictive techniques for a more accurate appraisal of the spiral groove face seal.

* It is recommended that effort be devoted to the development of a predictive analysis specifically modeled for the narrow land seal.

The experimental work of this contract demonstrated the feasibility of the spiral groove concept and its adaptability to the SNAP-8 alternator seal system. The attempt at long duration testing for the purpose of defining seal life and reliability was not successful. A further continuation of the experimental work would involve tests with selected seal materials over extended test periods.

* It is recommended that further effort be devoted to the selection of a suitable seal material to be used for extended duration testing under simulated SNAP-8 conditions. The actual materials used and the test times involved would be based on manufacturing considerations as well as SNAP-8 requirements.

APPENDIX A

This appendix concerns the time sharing computer program on the spiral groove bearing that has been used in this contract. The program is written in FORTRAN and has the following input variables:

Program Variable	Analysis Variable	Program Variable	Analysis Variable
ALF	α, degrees	A1IN	a_1
COTA	cot (α)	A2	a_2
TANA	tan (α)	DIN	D
RO	R_o	D2	d_2
R2	R_2	RHO	ρ
R3	R_3	XK	k
R4	R_4	HO	h_o
P1	P_1	E	η
OHM	ω		

(See nomenclature section IIB. for a further definition of these inputs).

These variables are to be entered in the above order starting with line number 10220 with the format shown in the listing.

The last variable to be entered is H2 (h_2). A series of values of H2 may be entered as the last line of data. (Note that line 10036 of the program determines the number and values for P2 which in turn determines the number of H2 values to be read in. In this listing P2 = PA = 6, 8, 10, 12 and 14 thus requiring 5 values for H2.)

Output:

The order of the outputs is given when the program first starts to run. For each case run, only the varying initial conditions are listed (see sample output, this appendix).

The actual output variables are:

Program Variable	Analysis Variable	Program Variable	Analysis Variable
D1	d_1	F4	F4
S SUB T	S_t	F	F
P3	P_3	W	W
F3	F_3		
FO	F_o		
F1	F_1		
F2	F_2		

(See nomenclature section IIB. for further definition.)

LISTING FOR
SPIRAL GROOVE COMPUTER PROGRAM

```
10000 READ, ALF,COTA,TANA,R0,R2,R3,R4
10005 READ,P1,OHM,A1IN,A2
10010 READ,DIN,D2,RH0,XK,H0,E
10015 PRINT, 1"   SPIRAL  GROOVE  BEARING"
10025 PRINT,1"  ORDER  OF  OUTPUT"
10030 PRINT,1"          D1      S SUB T         P3         F3          F0"
10035 PRINT,1"          F1              F2         F4          F             W"
10036 DO 100 P2=6,14,2
10037 P4=P2
10038 READ,H2
10040 PI= 3.14159
10042 PRINT,1"H2=",H2,"   P2=P4=",P2
10045 H1= H2+H0
10050 H= H2/H1
10055 V2=R2*OHM
10060 V3= R3*OHM
10065 GAM= A2/A1IN
10070 D=D2-.5*(A1IN*(1.-(ALF/90.))*TANA*((1.-H**3)/(1.+H**3)))
10075 DENOM= ((1.+GAM*H**3)*(GAM+H**3))+H**3*COTA**2*(1.+GAM)**2
10080 G1= GAM*H**2*COTA*(1.-H)*(1.-H**3)/DENOM
10085 G2= H**2*(1.+COTA**2)*(GAM+H**3)/DENOM
10090 A1= -GAM*(1.-H)*(1.+GAM*H**3)/DENOM
10095 C1= COTA*(1.+GAM)*(1.-H)*GAM*H**3/DENOM
10100 D0= (P2-P1)*H2**2/(6.*E*V2*G1)
10105 D1= D0+A1IN*(1.-ALF/90.)*TANA*((1.-H**3)/(1.+H**3))*(A1*COTA
10110 + /(A1*COTA+C1))
10115 SB= LOG(R4/R3)/(PI*D*V3*RH0*H2)+2.*G2/(V3*H1*A1IN*RH0*XK)
10120 SST= (G1+((P2-P4)*H2**2)/(6.*E*V3*D))/SB
10125 P3= P4+6.*E*SST*LOG(R4/R3)/(PI*RH0*H2**3)
10130 PART= (R4**2-R3**2)/4.-R4**2/2.*LOG(R4/R3)
10135 F3=PI*P3*(R4**2-R3**2)+(2.*PI*(P3-P4)/LOG(R4/R3))*PART
10140 F0= P1*PI*((R2-D1)**2-R0**2)
10145 F1=2.*P2*PI*D1*R2-(((3.*PI*E*OHM*R2**4)/(2.*H2**2))*(2.*D0
10150 + /R2)**2*G1)
10155 PT2= ((R3**2-(R2+DIN)**2)/4.-((R2+DIN)**2/2.*(LOG(R3/(R2+DIN
10160 + ))))*(1.+GAM)
10165 PT1= (12.*E*SST*G2/(RH0*H1*H2**2))*PT2
10170 PT0= (3.*PI*E*OHM*R3**4/(2.*H2**2))*(2.*D/R3)**2*G1
10175 F2= P3*PI*(R3**2-(R2+DIN)**2)-PT0-PT1
10180 F4= 2.*PI*R2*P2*DIN
10185 F= F0+F1+F2+F3+F4
10190 PT0= (P2+P3)*PI*R3*D2+((P3+P4)/2.)*PI*R4*(R4-R3)
10195 W= P1*PI*((R2-DIN)**2-R0**2)+P2*PI*R2*(D1+2.*DIN)+PT0
10200 PRINT 500,1 D1,SST,P3,F3,F0
10205 PRINT 500,1 F1,F2,F4,F,W
10210 500 FORMAT( 5F10.4)
10213 100 CONTINUE
10215 $DATA
10220 20,2.7475,.36397,1.066,1.203,1.268,1.316
10225 0,1255,.164,.06
10230 .025,.06,.0397,36,.004,.637E-06
10235 .00039,.00033,.00027,.00017,.00007
```

SAMPLE OUTPUT
SPIRAL GROOVE COMPUTER PROGRAM

```
RUN


SPIRL3      9:12    ST TUE 03/04/69


   SPIRAL  GROOVE  BEARING

  ORDER  OF  OUTPUT

        D1      S SUB T        P3         F3          F0

        F1            F2        F4          F            W

H2=  3.90000E-04   P2=P4=        6.00

     .0546      .0024   34.4087    4.9356      .0000

    2.2915   11.9345    1.1338   20.2954   14.6933

H2=  3.30000E-04   P2=P4=        8.00

     .0568      .0015   38.0236    5.6236      .0000

    3.1221   13.4592    1.5117   23.7166   17.2627

H2=  2.70000E-04   P2=P4=       10.00

     .0588      .0009   41.6347    6.3112      .0000

    3.9776   14.9732    1.8897   27.1516   19.8560

H2=  1.70000E-04   P2=P4=       12.00

     .0602      .0002   46.3156    7.1291      .0000

    4.8350   16.8388    2.2676   31.0705   22.7770

H2=  7.00000E-05   P2=P4=       14.00

     .0613      .0000   51.0368    7.9519      .0000

    5.7006   18.6899    2.6455   34.9879   25.7188


AT LINE NO. 10215: STOP  END

USED      11.83 UNITS.
```

Table D-1

SPIRAL GROOVE SHUTDOWN SEAL: 50-HOUR CONTINUOUS TEST--SNAP 8

			Anti-drive End											Drive End										
Time	rpm	Sump Temp °F (°F)	Bear. Temp (°F)	Oil Inlet (psig)	Oil Inlet (°F)	Cavity in. Hg Vac	Inbd Oil Outlet (°F)	Inbd Sling in. Hg Vac	Otbd Oil Outlet (°F)	Otbd Sling in. Hg Vac	S. G. S. Dif (psi)	Flow (gpm)	Otbd Trap Level (mm)	Bear. Temp (°F)	Oil Inlet (psig)	Cavity in. Hg Vac	Oil Outlet (°F)	Inbd Sling in. Hg Vac	Otbd Sling in. Hg Vac	Flow (gpm)	Gen Cavity in. Hg Vac	Sump in. Hg Vac	Face Seal in. Hg Vac	Pump Disch (psig)
1030	12040	243	275	0	220	26.7	273	1.0	257	10.8	9.6	0.32	10.0	255	0	16.0	244	9.0	15.0	0.32	30+	20.5	10.5	35
1100[1]	12020	238	280	0	223	26.6	280	1.5	257	11.0	9.6	.32	10.0	261	0	16.5	248	10.5	15.5	.32	30+	20.5	10.0	36
1130	12000	233	280	0	220	26.4	280	1.7	257	10.5	9.9	.32	10.0	257	0	17.0	244	11.2	15.5	.32	30+	20.4	13.2	36
1200	12040	234	280	0	220	26.5	279	1.8	259	11.0	9.6	.32	10.0	259			244				30+	20.6		
1230	12020	236	282	0	221	26.5	282	2.1	260	10.0	10.2	.32	10.0	259	0	17.1	242	11.1	15.5	.32	30+	20.5	13.2	36
1300	12020	237	284	0	223	26.5	282	2.0	264	10.5	9.9	.32	10.0	259	0	17.1	244	11.1	15.5	.32	30+	20.5	13.2	36
1330	12040	237	284	0	223	26.5	284	2.2	264	10.5	10.0	.32	10.0	259	0	17.2	248	11.0	15.5	.32	30+	20.4	13.2	36
1400	12020	237	284	0	223	26.5	284	2.0	264	10.5	9.8	.32	10.0	259	0	17.2	248	11.2	15.5	.32	30+	20.5	13.5	36
1430	12020	238	285	0	225	26.2	284	2.0	266	11.0	9.9	.32	10.0	262	0	17.2	248	11.2	15.5	.32	30+	20.5	13.5	36
1530	12040	240	288	0	226	26.2	288	2.2	266	10.8	9.9	.32	10.0	258	0	17.8	248	11.5	15.6	.32	30+	20.5	13.5	36
1600	12040	230	280	0	220	26.1	280	2.2	257	11.0	10.0	.32	10.0	258	0	17.8	243	11.5	15.6	.32	30+	20.5	13.5	35
1630	12040	236	282	0	221	26.1	282	1.8	260	11.5	9.7	.32	10.0	259	0	17.5	244	11.5	15.6	.32	30+	20.6	14.0	34
1700	12020	240	286	0	222	26.1	282	1.8	260	11.0	10.1	.32	10.0	260	0	17.5	244	11.5	15.6	.32	30+	20.5	14.0	35
1730	12040	240	286	0	224	26.1	287	2.0	268	11.2	9.5	.32	10.0	264	0	18.0	248	11.6	15.6	.32	30+	20.5	14.0	35
1800	12040	232	286	0	223	26.5	287	2.0	264	11.5	9.8	.32	10.0	260	0	17.9	248	11.6	15.6	.32	30+	20.5	14.0	36
1830	12040	235	278	0	212	26.5	278	2.0	257	11.0	10.1	.32	10.0	253	0	17.9	239	11.2	15.6	.32	30+	20.5	13.0	36
1900	12020	244	283	0	223	26.5	283	1.8	262	11.2	9.8	.32	10.0	257	0	17.9	244	11.2	15.6	.32	30+	20.4	13.0	36
1930	12020	246	288	0	226	26.6	286	2.0	266	11.0	9.7	.32	10.0	262	0	17.5	248	11.8	15.5	.32	30+	20.5	13.0	35
2000	12040	242	282	0	219	26.0	282	2.2	266	10.8	10.0	.32	10.0	257	0	17.5	242	11.0	15.6	.32	30+	20.5	12.8	36
2030[2]	12040	238	284	0	224	26.0	284	2.0	262	11.2	9.7	.32	10.0	257	0	17.2	244	11.0	15.6	.32	30+	20.5	13.0	35
2100	12040	236	284	0	221	26.0	284	2.0	266	11.5	9.8	.32	10.0	260	0	17.5	246	11.5	15.6	.32	30+	20.5	13.0	35
2130	12020	234	284	0	221	26.0	284	2.2	264	11.0	10.0	.32	10.0	260	0	17.5	245	11.5	15.6	.32	30+	20.5	13.0	35
2200	12020	227	283	0	219	26.0	280	2.4	264	10.8	10.2	.32	10.0	257	0	17.6	243	11.2	15.6	.32	30+	20.4	13.0	35
2230	12040	230	284	0	221	26.0	284	2.0	266	11.5	9.6	.32	10.0	259	0	17.6	246	11.2	15.6	.32	30+	20.5	13.0	35
2300	12020	228	284	0	221	26.0	284	2.0	263	11.0	10.0	.32	10.0	259	0	17.6	246	11.5	15.6	.32	30+	20.5	13.0	35
2400	12020	228	282	0	221	26.0	284	2.0	260	11.0	9.9	.32	10.0	260	0	17.6	244	11.5	15.6	.32	30+	20.5	13.0	35
0100	12040	228	282	0	221	26.0	282	2.0	264	11.0	10.0	.32	10.0	260	0	17.6	244	11.5	15.6	.32	30+	20.5	13.0	35
0200	12040	228	282	0	221	26.0	284	2.0	264	11.0	10.0	.32	10.0	260	0	17.6	244	11.5	15.6	.32	30+	20.5	13.0	35
0300	12020	228	282	0	222	26.0	284	2.0	262	11.0	10.0	.32	10.0	261	0	17.6	244	11.5	15.6	.32	30+	20.5	13.0	35
0400	12040	226	282	0	221	26.0	280	2.0	262	11.0	10.0	.32	10.0	258	0	17.6	244	11.5	15.6	.32	30+	20.5	13.0	35
0500	12020	226	282	0	221	26.0	282	2.0	261	11.0	9.9	.32	10.0	258	0	17.6	244	11.5	15.6	.32	30+	20.5	13.0	35
0600	12040	228	284	0	222	26.0	282	2.0	261	11.0	10.0	.32	10.0	258	0	17.6	244	11.5	15.6	.32	30+	20.5	13.0	35
0700	12040	226	283	0	221	26.0	282	2.1	261	11.0	10.0	.32	10.0	259	0	17.4	244	11.5	15.6	.32	30+	20.5	13.0	35
0800	12040	225	283	0	221	26.0	284	2.2	261	11.0	10.0	.32	10.0	257	0	17.4	244	11.5	15.6	.32	30+	20.5	13.0	35

TABLE D-1 contd

0900	12060	224	284	0	221	25.8	284	2.3	262	11.0	9.9	0.32	10.0	259	0	17.6	246	11.6	15.6	0.32	30+	20.5	13.0	35.0
1000	12020	225	284	0	221	26.0	284	2.3	264	10.8	10.2	.32	10.0	259	0	17.6	246	11.5	15.6	.32	30+	20.5	13.0	35.0
1100[3]	12020	225	284	0	223	26.0	282	2.0	262	11.2	9.8	.32	10.0	260	0	17.6	248	11.5	15.6	.32	30+	20.5	13.0	35.0
1200	12040	226	287	0	224	26.0	286	2.0	266	11.5	9.8	.32	10.0	262	0	17.6	250	11.9	15.6	.32	30+	20.5	13.0	35.0
1300	12020	224	284	0	225	26.0	284	1.9	264	11.5	9.7	.32	10.0	264	0	17.6	248	11.9	15.6	.32	30+	20.5	13.2	35.0
1400	12040	225	287	0	225	26.2	286	1.8	266	11.8	9.4	.32	10.0	262	0	17.6	252	11.7	15.6	.32	30+	20.4	13.2	35.0
1500	12020	225	288	0	225	26.0	286	2.3	266	10.8	9.8	.32	10.0	266	0	17.6	250	11.8	15.6	.32	30+	20.5	13.2	35.0
1600	12020		284	0	221	26.0	284	2.0	263	11.2	9.8	.32	10.0	259	0	17.6	246	12.2	15.6	.32	30+	20.5	13.2	35.0
1700	12020	225	285	0	224	26.0	284	2.0	262	11.0	10.0	.32	10.0	262	0	17.6	248	12.2	15.6	.32	30+	20.5	13.2	35.0
1800	12040	215	280	0	219	26.0	279	2.0	258	11.0	9.9	.32	10.0	255	0	17.6	243	12.0	15.6	.32	30+	20.5	13.2	35.0
1900	12060	215	280	0	219	26.0	279	2.2	259	11.0	9.8	.32	10.0	256	0	17.6	243	12.0	15.6	.32	30+	20.5	13.0	35.0
2000	12040	215	284	0	221	26.0	282	2.0	264	11.0	9.8	.32	10.0	259	0	17.6	246	12.0	15.4	.32	30+	20.5	13.0	35.0
2100	12040	215	284	0	221	26.0	284	2.0	262	11.5	9.4	.32	10.0	259	0	17.5	246	12.0	15.4	.32	30+	20.5	13.0	35.0
2200[4]	12020	215	284	0	221	25.8	284	2.4	262	10.3	10.0	.32	10.0	259	0	17.5	246	12.0	15.4	.32	30	20.5	13.0	35.0
2300	12040	212	284	0	221	25.8	282	2.4	262	11.0	9.8	.32	10.0	259	0	17.5	246	12.2	15.5	.32	30	20.5	13.0	35.0
2400	12060	212	284	0	221	25.8	282	2.6	260	11.0	9.9	.32	10.0	259	0	17.5	246	11.5	15.4	.32	30	20.5	13.0	35.0
0100	12040	212	284	0	220	25.5	282	2.5	259	10.9	9.8	.32	10.0	257	0	17.5	242	11.8	15.4	.32	30	20.5	13.0	35.0
0200	12020	212	284	0	221	25.5	281	2.4	260	10.9	9.9	.32	10.0	258	0	17.0	242	12.0	15.4	.32	30-	20.5	13.0	35.0
0300	12020	200	284	0	221	25.2	280	2.5	260	10.3	10.1	.32	10.0	256	0	17.1	244	12.0	15.2	.32	30-	20.5	13.0	35.0
0400	12020	198	284	0	221	25.2	281	2.5	260	10.2	10.0	.32	10.0	257	0	17.1	245	12.0	15.2	.32	30-	20.5	13.0	35.0
0500	12040	190	284	0	221	25.2	281	2.5	260	10.2	10.1	.32	10.0	257	0	17.1	244	12.0	15.2	.32	30-	20.5	13.0	35.0
0600	12040	185	284	0	221	25.2	281	2.5	262	10.2	10.1	.32	10.0	257	0	17.1	244	12.0	15.2	.32	30-	20.5	13.0	35.0
0700	12020	185	287	0	223	25.2	282	2.5	264	10.2	10.1	.32	10.0	258	0	17.1	246	12.0	15.2	.32	30-	20.5	13.0	35.0
0800	12040	185	284	0	221	25.2	282	2.5	260	10.2	10.1	.32	10.0	255	0	17.0	244	12.0	15.2	.32	30-	20.5	13.0	35.0
0900	12040	185	286	0	224	25.2	284	2.5	264	10.2	10.1	.32	10.0	259	0	17.0	246	12.0	15.1	.32	30-	20.5	13.0	35.0
1000	12040	190	288	0	225	25.2	286	2.3	266	10.5	10.0	.32	10.0	260	0	17.0	248	12.0	15.0	.32	30-	20.5	13.0	35.0
1100	12040	187	288	0	225	25.5	286	2.5	266	10.5	9.9	.32	10.0	260	0	17.0	248	12.5	15.2	.32	30-	20.5	13.0	35.0
1200[5]	12020	186	284	0	223	25.5	282	2.3	264	10.5	9.9	.32	10.0	262	0	17.0	248	12.5	15.2	.32	30-	20.5	13.2	35.0
1300	12040	185	284	0	221	25.5	282	2.5	262	10.2	10.1	.32	10.0	259	0	17.0	246	12.5	15.2	.32	30-	20.5	13.2	35.0
1325	12040	185	284	0	221	25.5	282	2.5	261	10.2	10.1	.32	10.0	260	0	17.0	247	12.5	15.2	.32	30-	20.5	13.2	35.0
1326	Termination																							

NOTES: The following Barometer and Ambient Temperature Data Corresponds to Superscrits Located in Time Column of Above Table:

1. Bar. = 29.92 in. Hg Amb. = 81°F
2. Bar. = 29.82 in. Hg Amb. = 81°F
3. Bar. = 29.91 in. Hg Amb. = 83°F
4. Bar. = 29.62 in. Hg Amb. = 83°F
5. Bar. = 29.48 in. Hg Amb. = 83°F

FIGURES

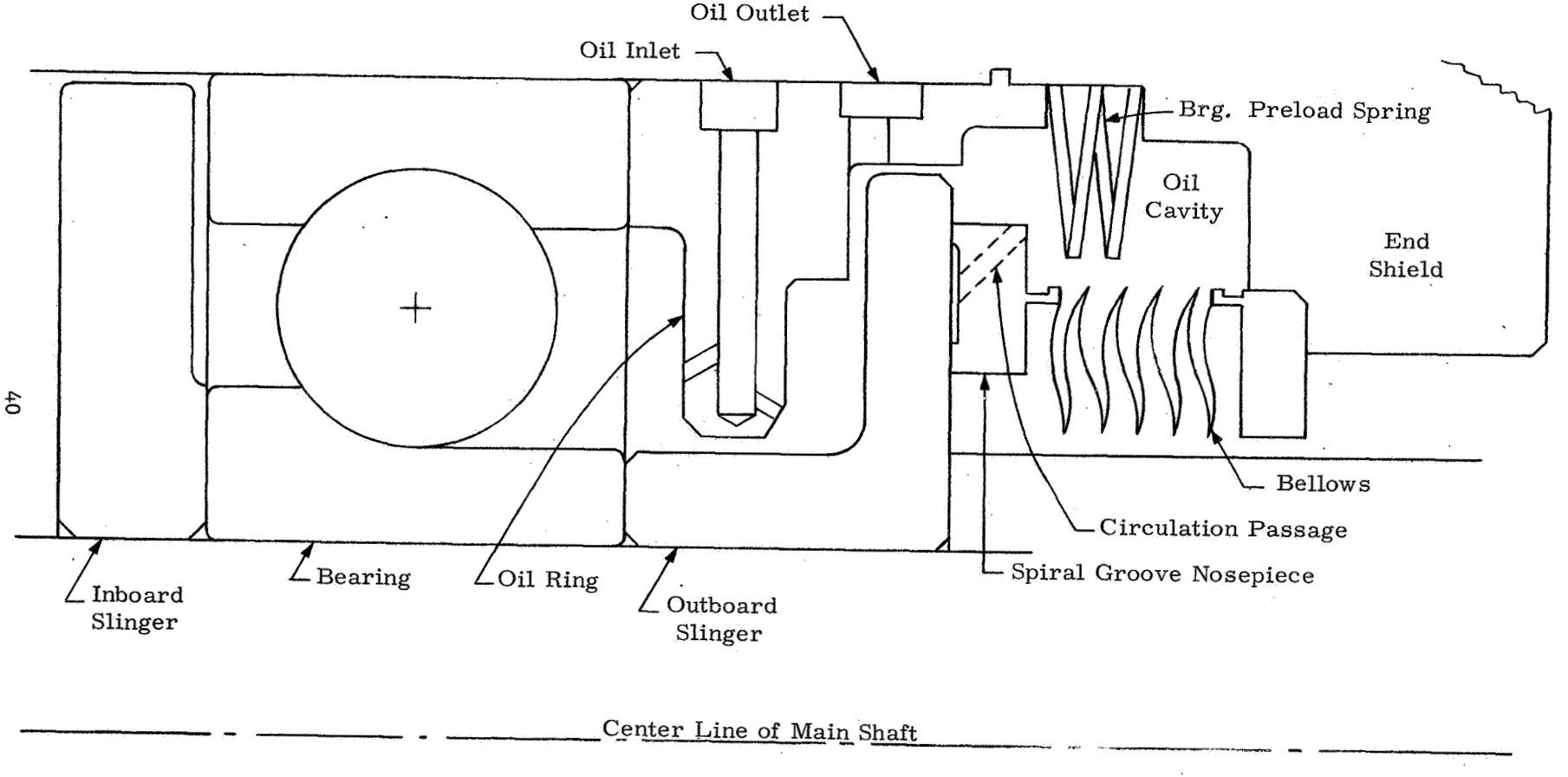

Figure 1 Schematic of Recirculating Design

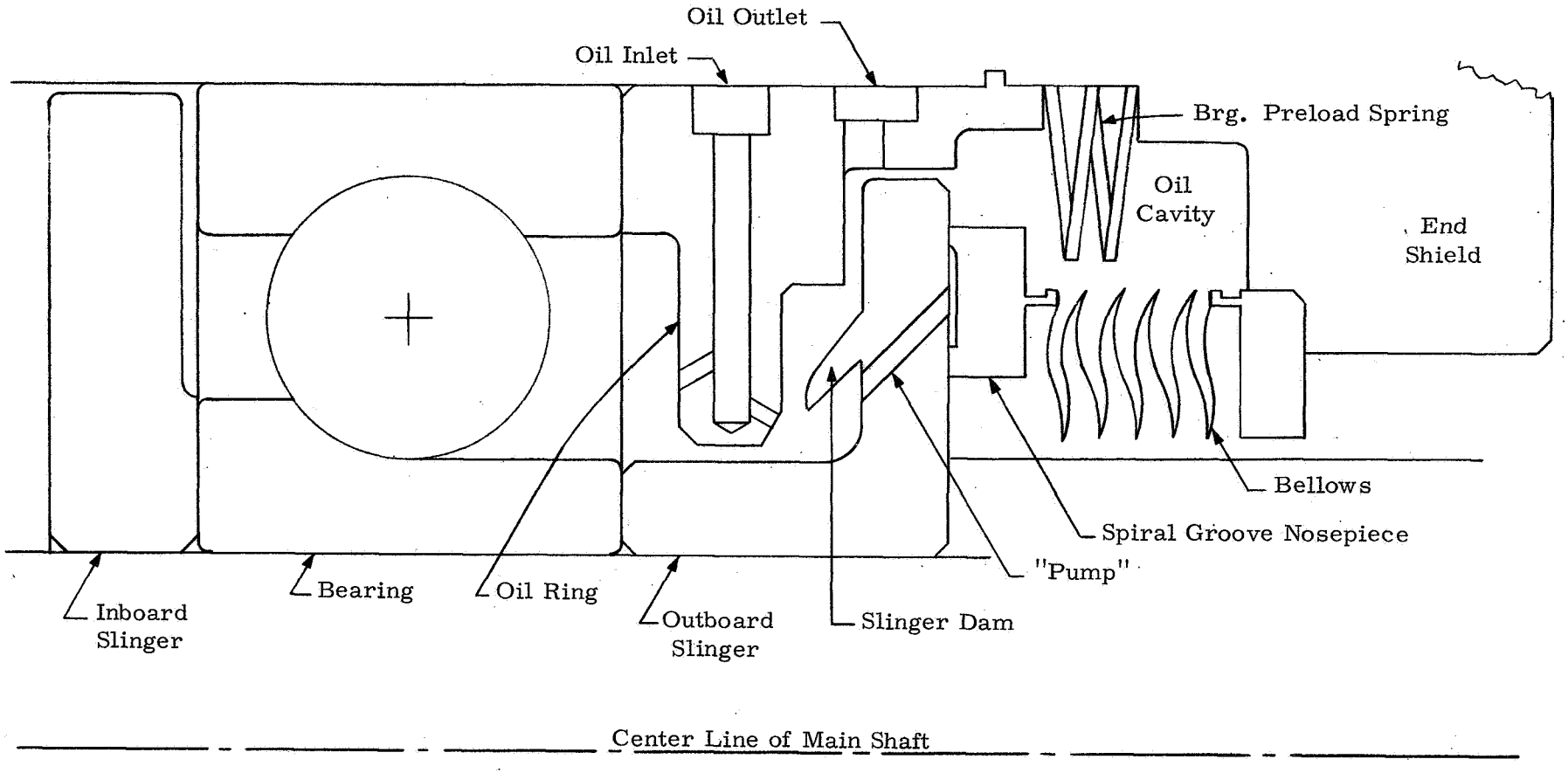

Figure 2. Schematic Positive Feed Design

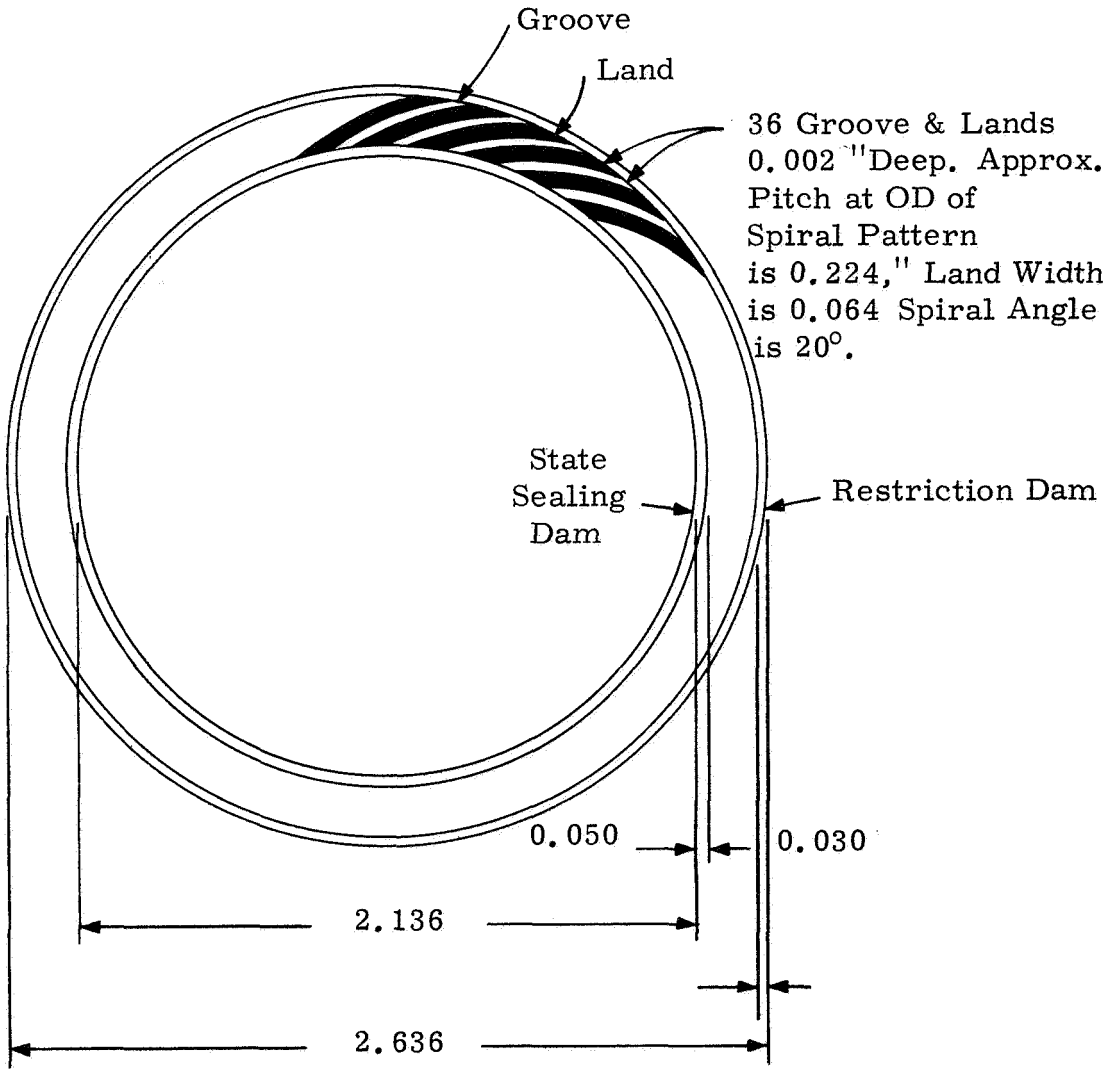

Coordinates for Spiral Groove Contour

Degree	Radius	Degree	Radius
0	1.1180	15	1.2331
3	1.1396	18	1.2535
5	1.1541	20	1.2689
7	1.1688	22	1.2857
10	1.1912	23	1.2936
12	1.2064		

Figure 3 Detail of Spiral Groove Pattern and Dams

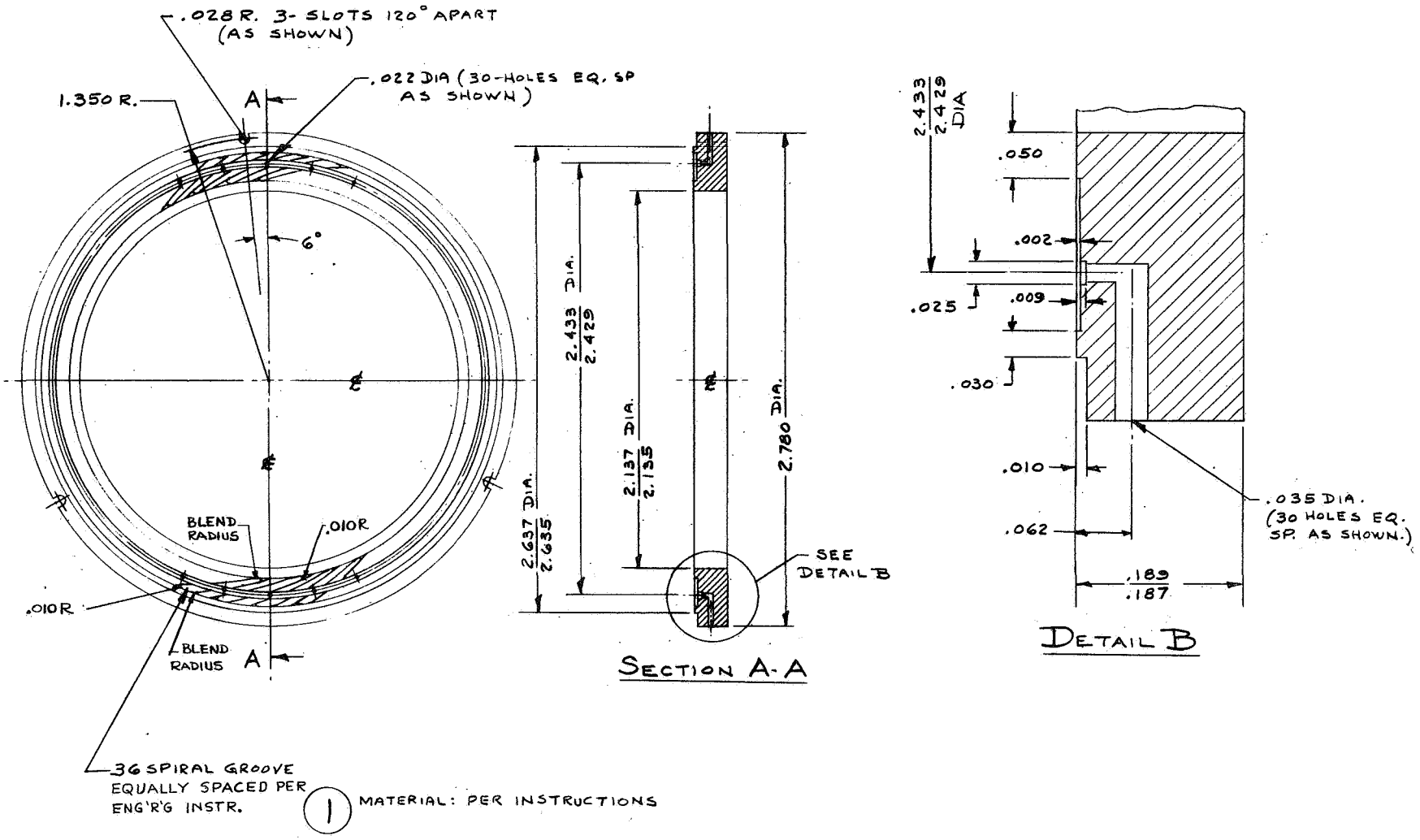

Figure 4 Seal Nose Piece

Figure 5 SNAP-8 Spiral Groove Seal Extended View

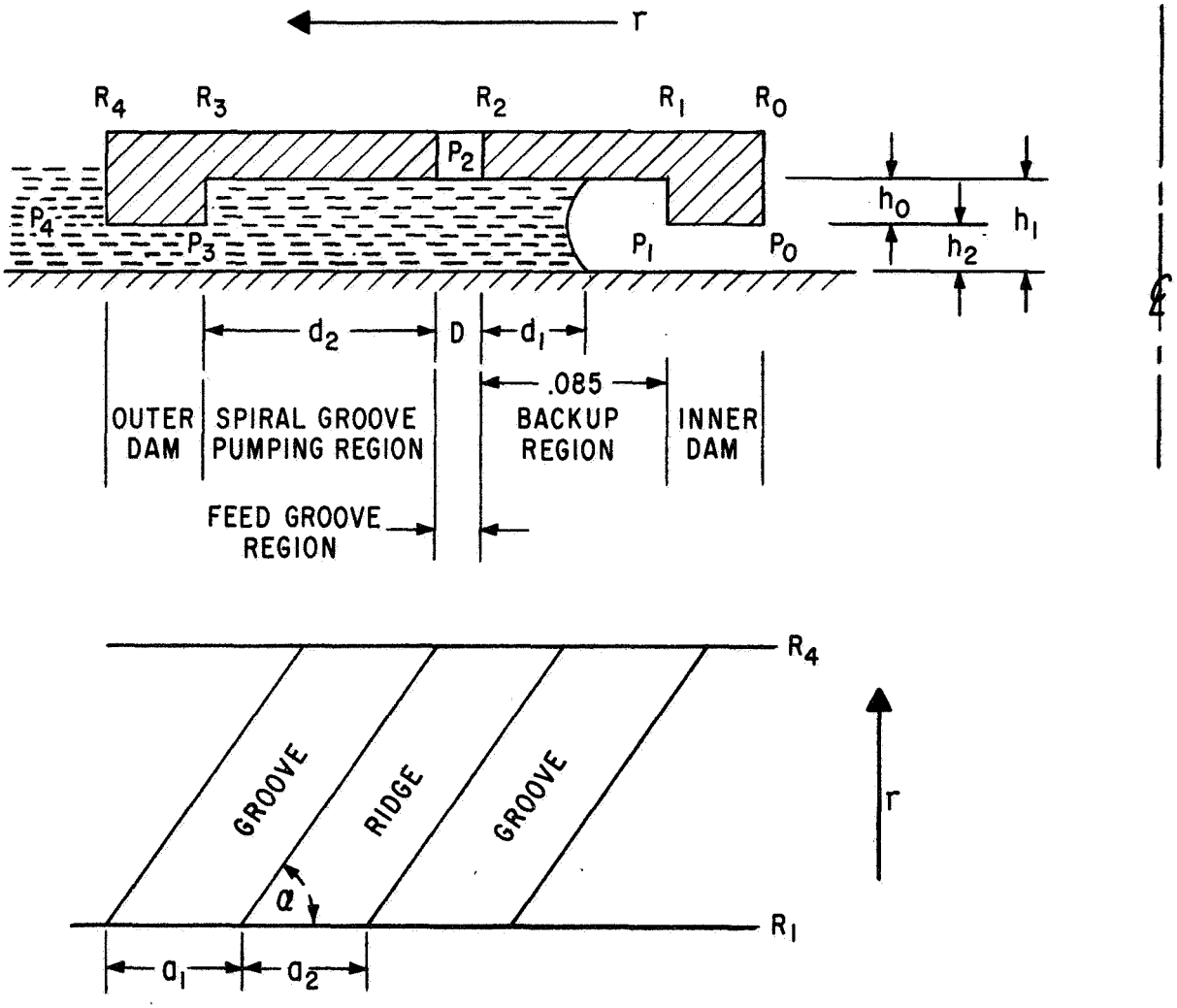

Figure 6 Spiral Groove Face seal Geometry.

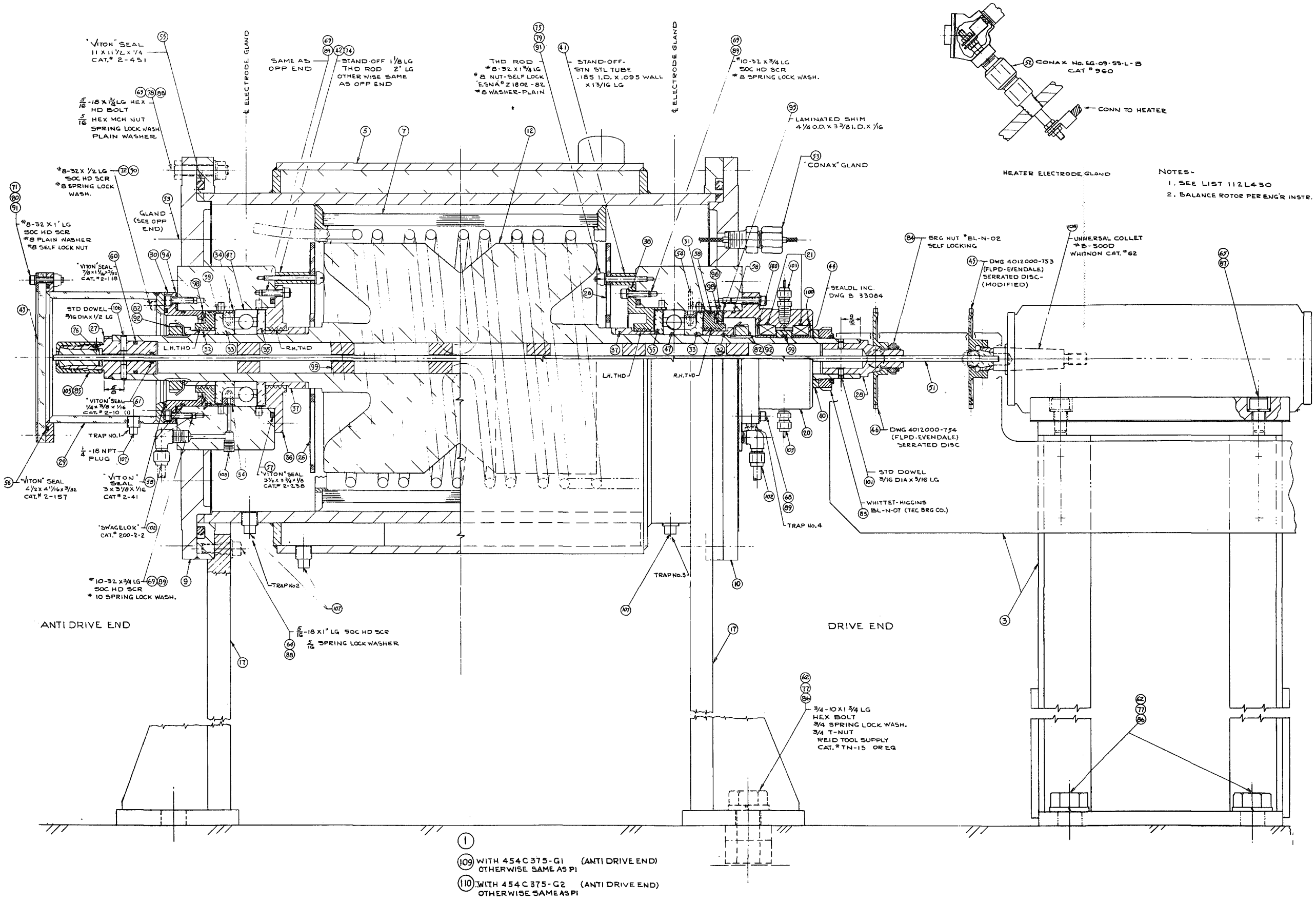

Figure 7 SNAP-8 Rotor and Casing Assembly Alternator Test (Unmodified)

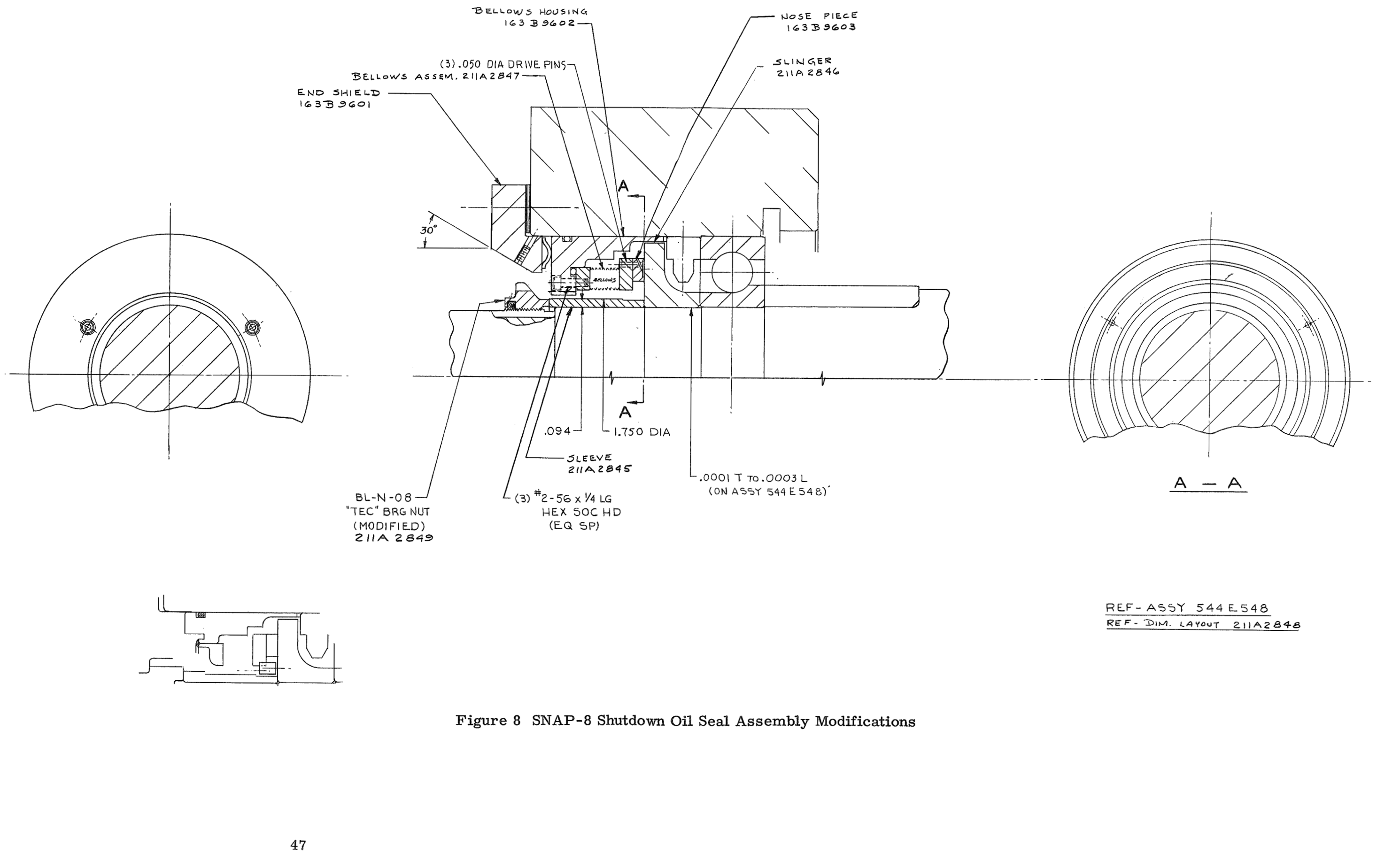

Figure 8 SNAP-8 Shutdown Oil Seal Assembly Modifications

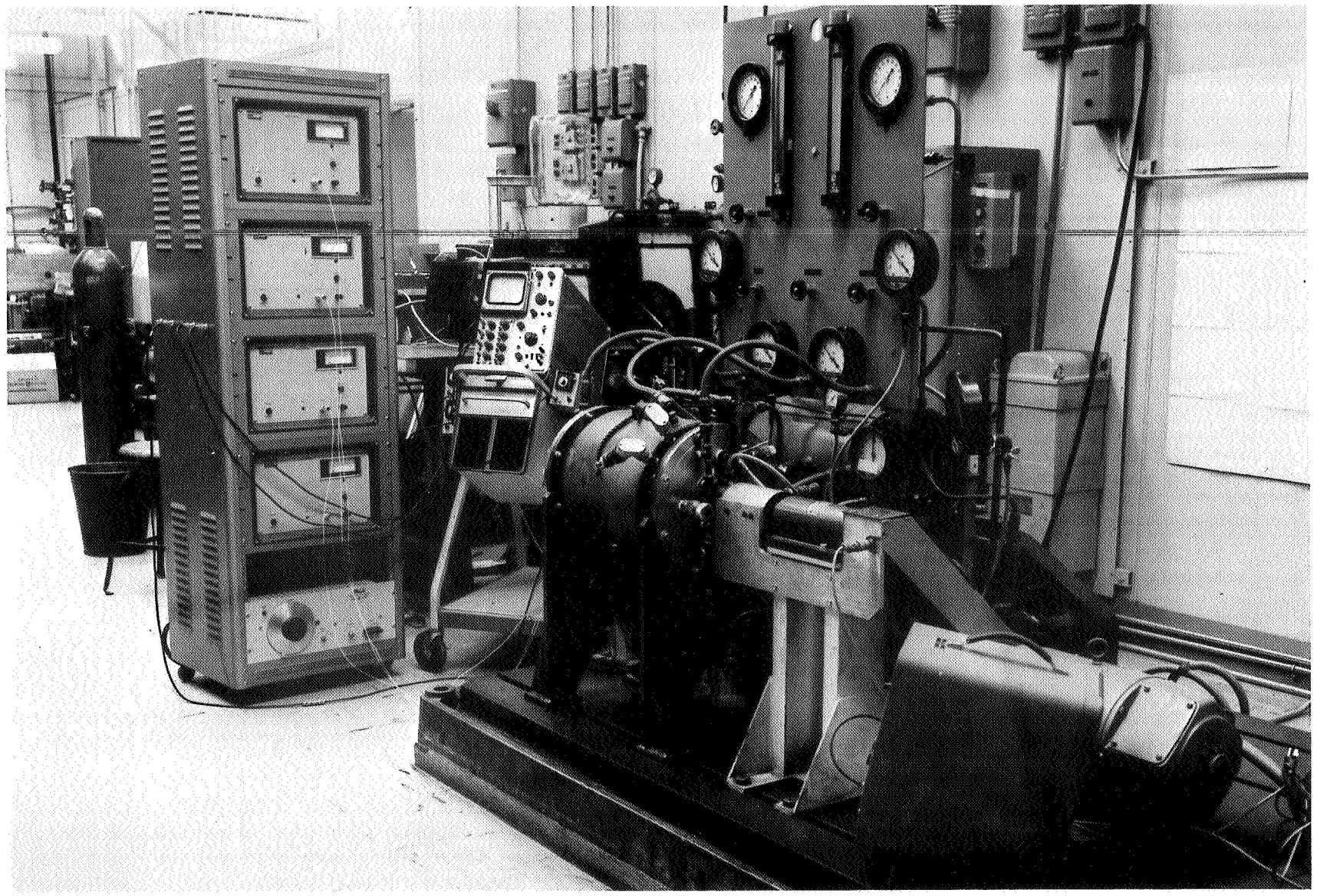

Figure 9 SNAP-8 Alternator Test Assembly

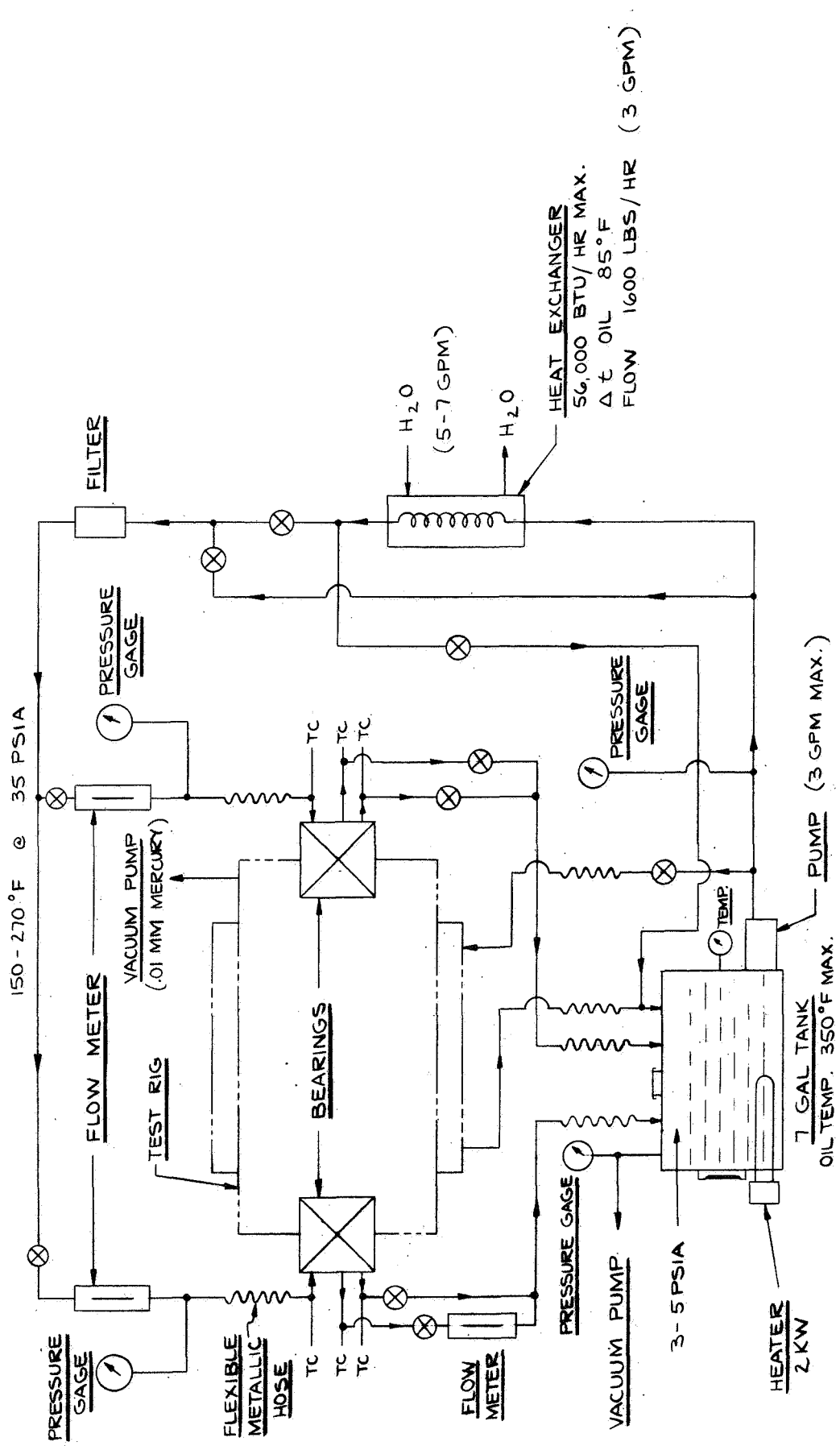

Figure 10 Lube System

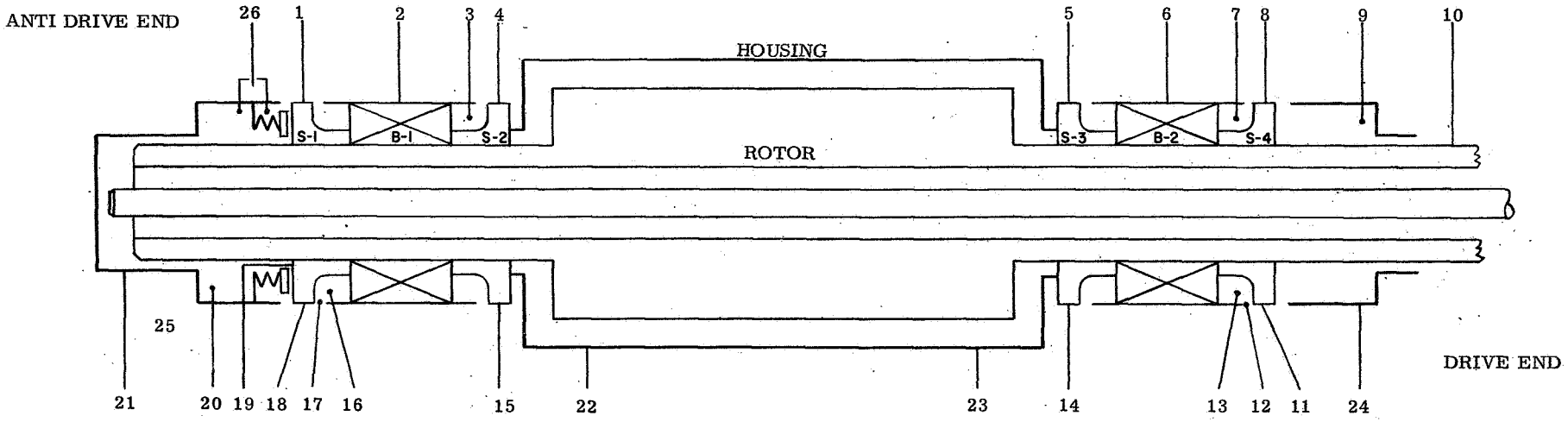

1. Outlet pressure slinger S-1
2. Bearing outer race temp B-1 BRG(3)
3. Cavity pressure B-1 BRG.
4. Outlet pressure slinger S-2
5. Outlet pressure slinger S-3
6. Bearing outer race temp B-2 BRG (3)
7. Cavity pressure B-2 BRG
8. Outlet pressure slinger S-4
9. End pressure B-2
10. Shaft speed
11. Outlet lube temp. slinger S-4
12. Inlet flow BRG. B-2
13. Inlet lube temp. BRG B-2
14. Outlet temperature slinger S-3
15. Outlet temperature slinger S-2
16. Inlet flow BRG. B-1
17. Inlet lube temp. BRG. B-1
18. Outlet temperature slinger S-1
19. End pressure B-1
20. Trap No. 1
21. Trap No. 2
22. Trap No. 3
23. Trap No. 4
24. Capacitance probe (3)
25. Seal differential pressure

Figure 11 Instrumentation Schematic

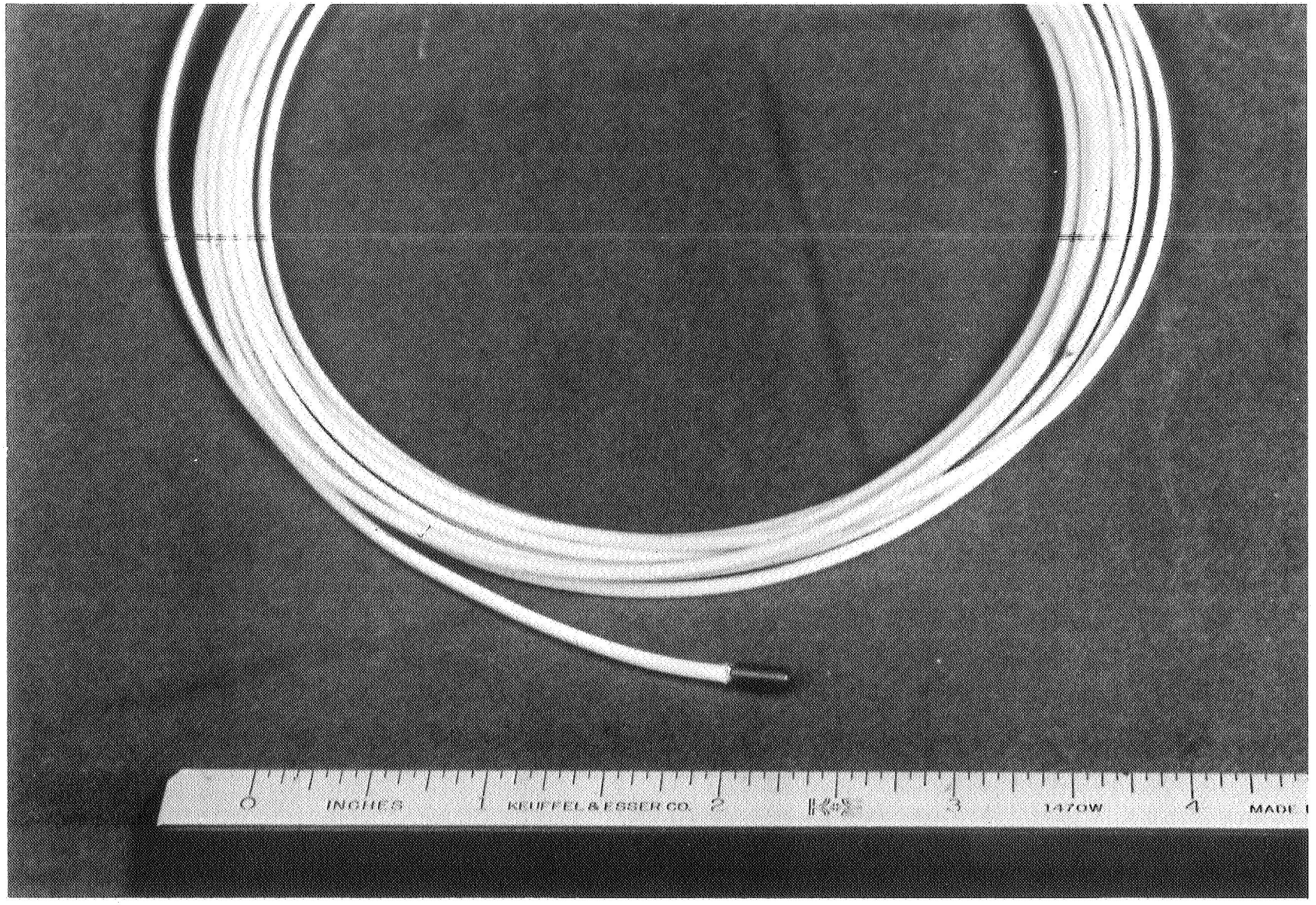

Figure 12 Capacitive Transducer and Coaxial Cable

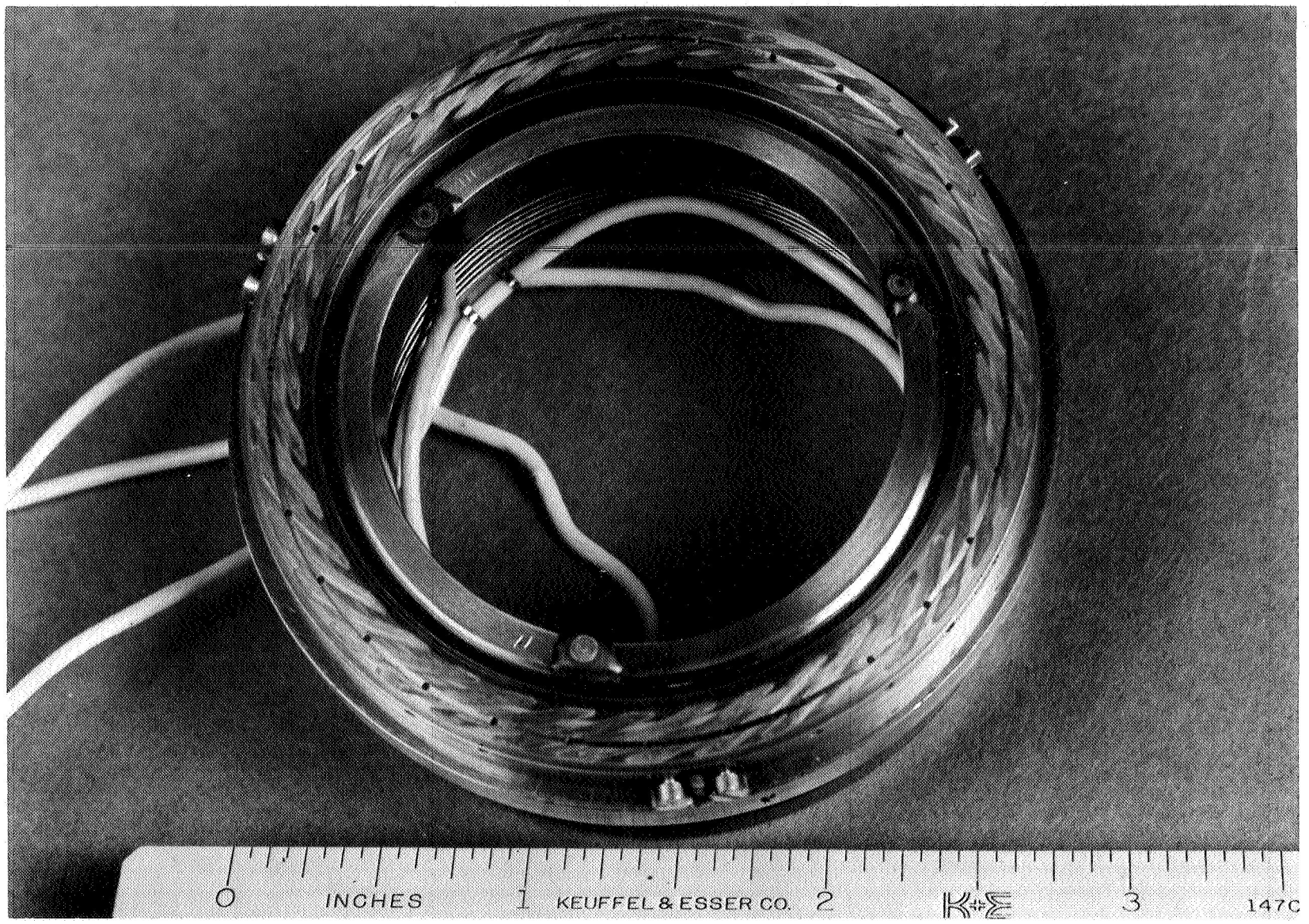

Figure 13 Seal Capacitive Probes

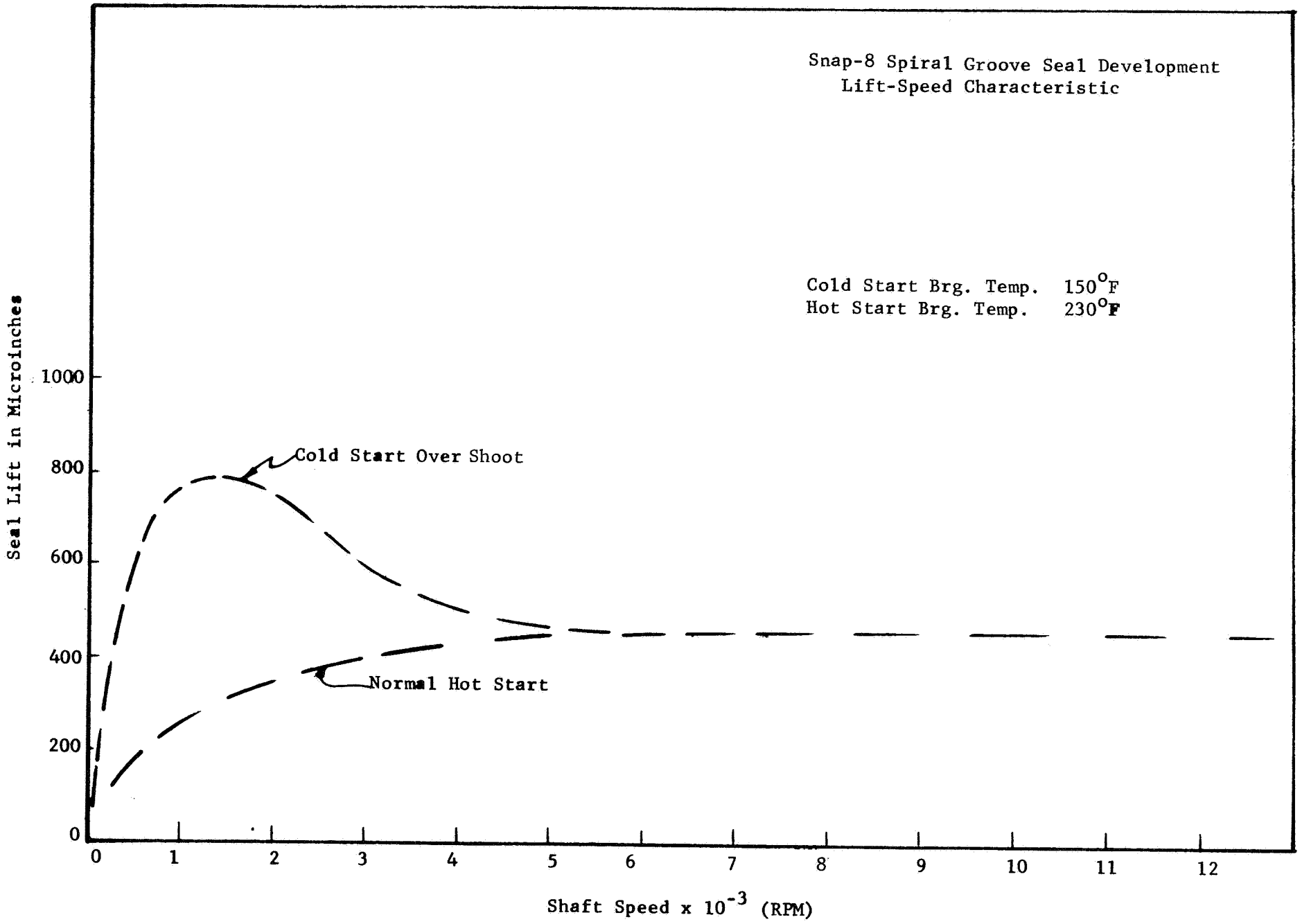
Snap-8 Spiral Groove Seal Development
Lift-Speed Characteristic
Cold Start Brg. Temp. 150°F
Hot Start Brg. Temp. 230°F
Seal Lift in Microinches
1000
800
600
400
200
0
Cold Start Over Shoot
Normal Hot Start
0
1
2
3
4
5
6
7
8
9
10
11
12
Shaft Speed x 10^{-3} (RPM)

Figure 14

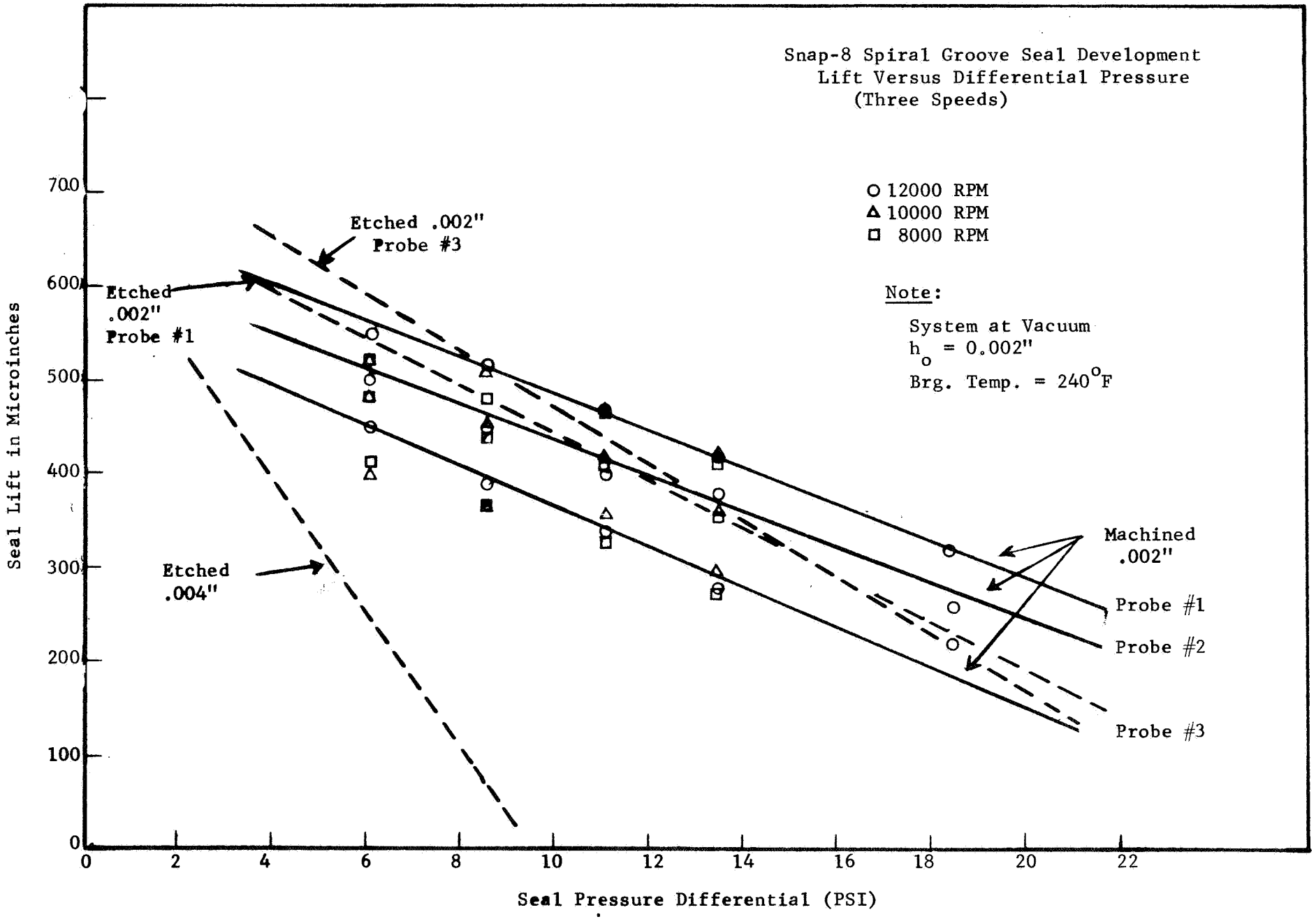
Snap-8 Spiral Groove Seal Development
Lift Versus Differential Pressure
(Three Speeds)
O 12000 RPM
Δ 10000 RPM
□ 8000 RPM
Note:
System at Vacuum
h_o = 0.002"
Brg. Temp. = 240°F
Etched .002"
Probe #3
Etched
.002"
Probe #1
Etched
.004"
Machined
.002"
Probe #1
Probe #2
Probe #3
Seal Lift in Microinches
Seal Pressure Differential (PSI)
0
100
200
300
400
500
600
700
0
2
4
6
8
10
12
14
16
18
20
22

Figure 15

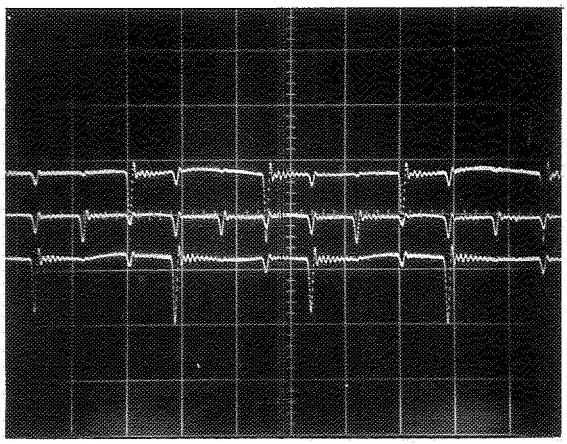

ΔP = 6.2 PSI

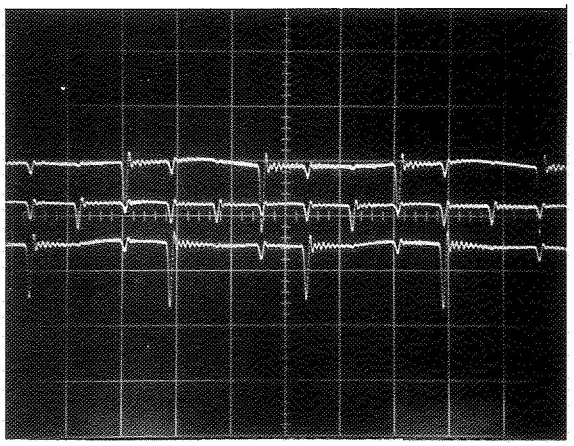

ΔP = 8.6 PSI

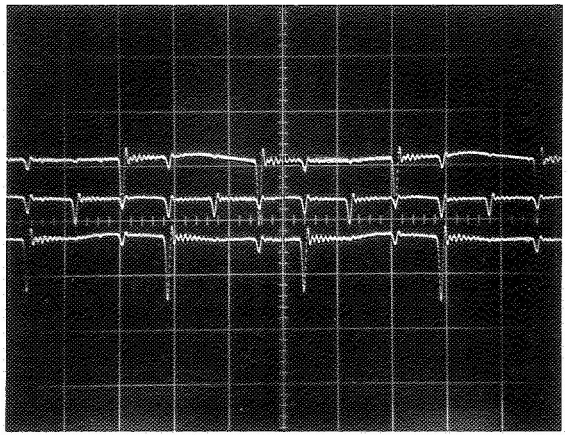

ΔP = 11.1 PSI

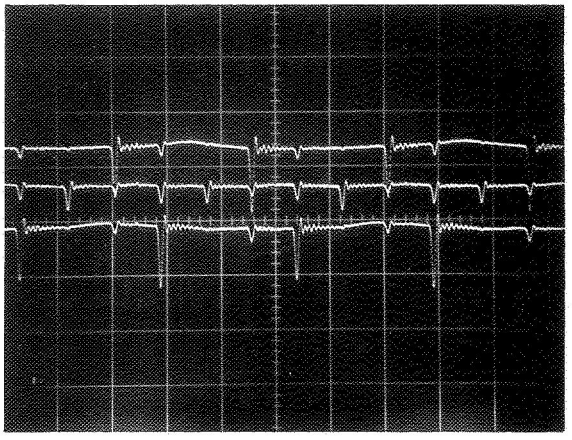

ΔP = 13.5 PSI

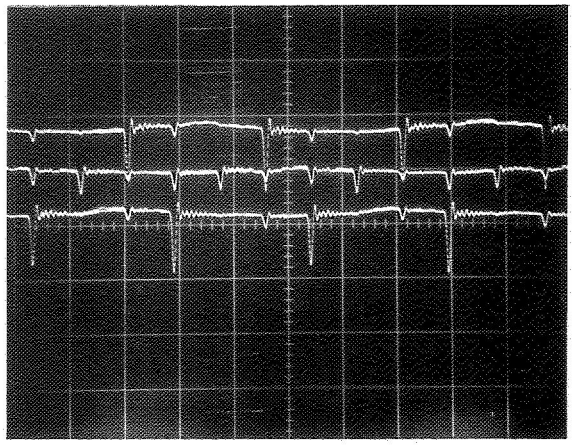

ΔP = 18.4 PSI

Figure 16

Capacitance Probe Oscillograph Trace

Speed = 12000 RPM
h_o = 0.002"
System at Vacuum
Seal ΔP as Noted
(Data Taken 2-5-69)

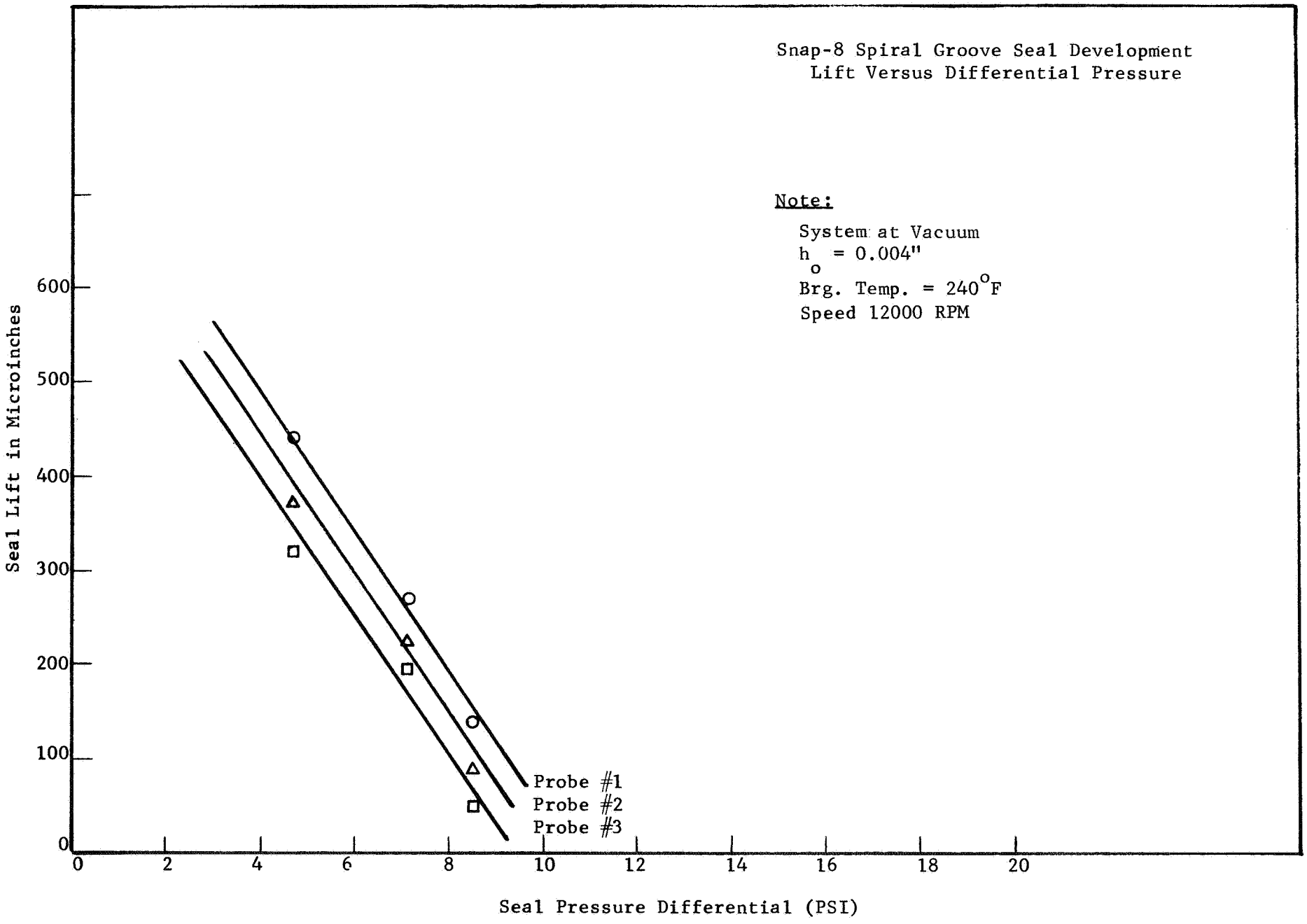
Snap-8 Spiral Groove Seal Development
Lift Versus Differential Pressure
Note:
System at Vacuum
h o = 0.004"
Brg. Temp. = 240°F
Speed 12000 RPM
Seal Lift in Microinches
0
100
200
300
400
500
600
0
2
4
6
8
10
12
14
16
18
20
Seal Pressure Differential (PSI)
Probe #1
Probe #2
Probe #3

Figure 17

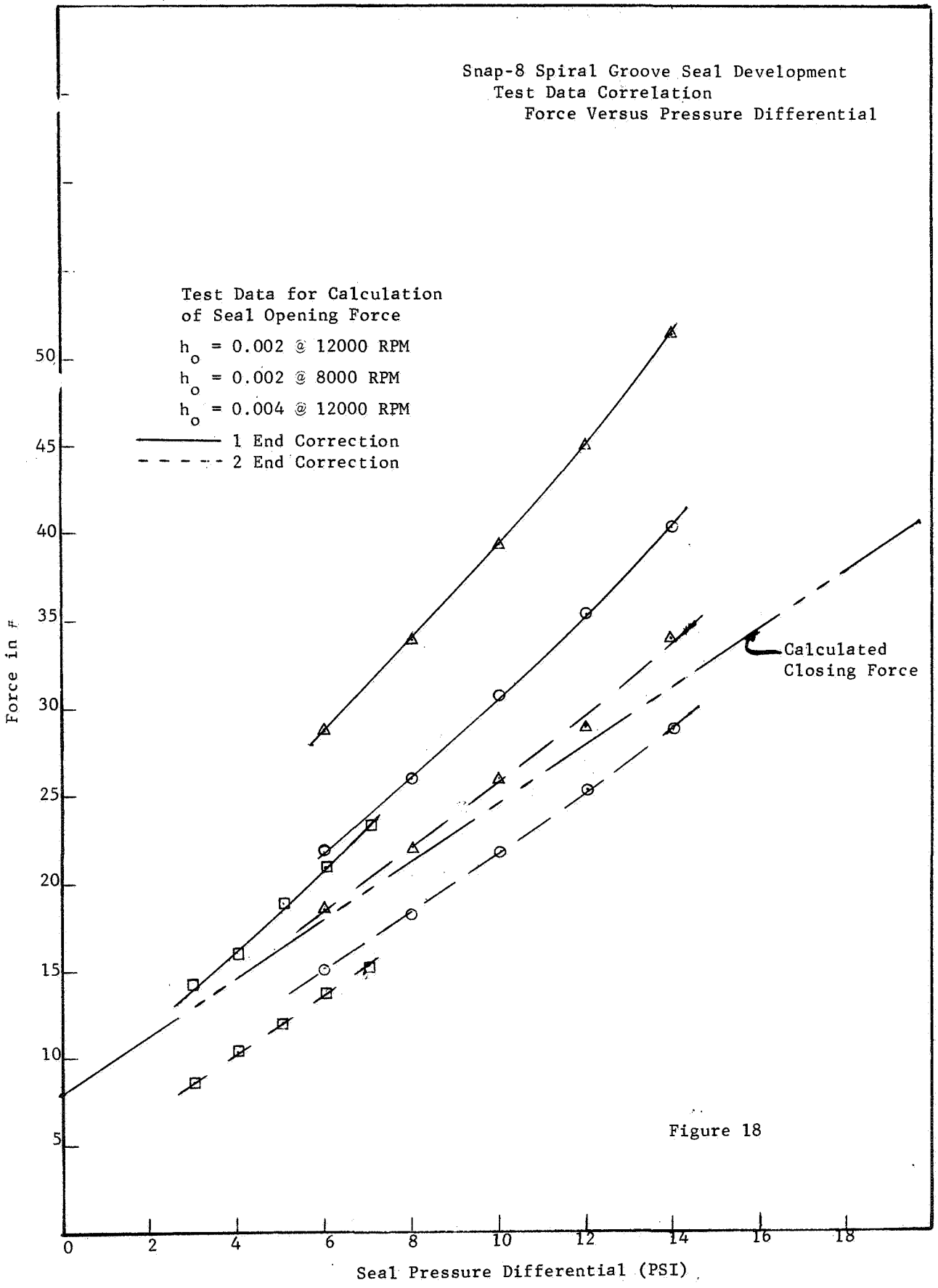
Snap-8 Spiral Groove Seal Development
Test Data Correlation
Force Versus Pressure Differential
Test Data for Calculation
of Seal Opening Force
h_o = 0.002 @ 12000 RPM
h_o = 0.002 @ 8000 RPM
h_o = 0.004 @ 12000 RPM
1 End Correction
2 End Correction
Calculated
Closing Force
Force in #
Seal Pressure Differential (PSI)
0
2
4
6
8
10
12
14
16
18
5
10
15
20
25
30
35
40
45
50

Figure 18

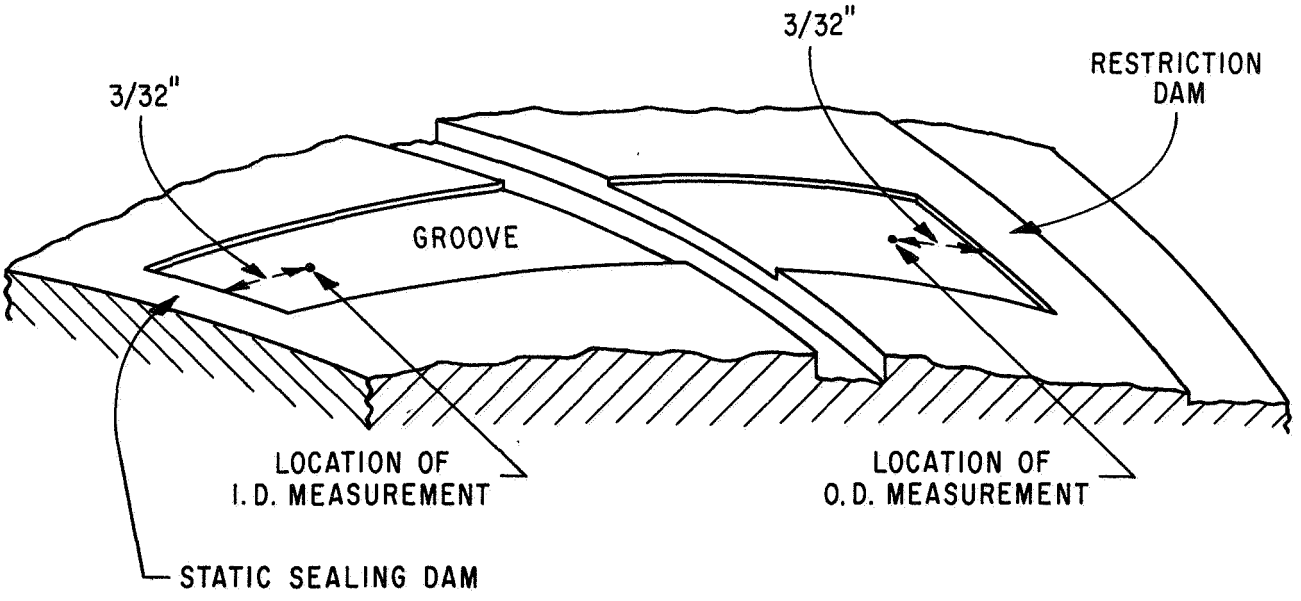

See Figure 4 for complete seal configuration

See **Table** 2 and Table 3 for values

DEPTH MEASUREMENT LOCATION

TYPICAL GROOVE

FIGURE 19

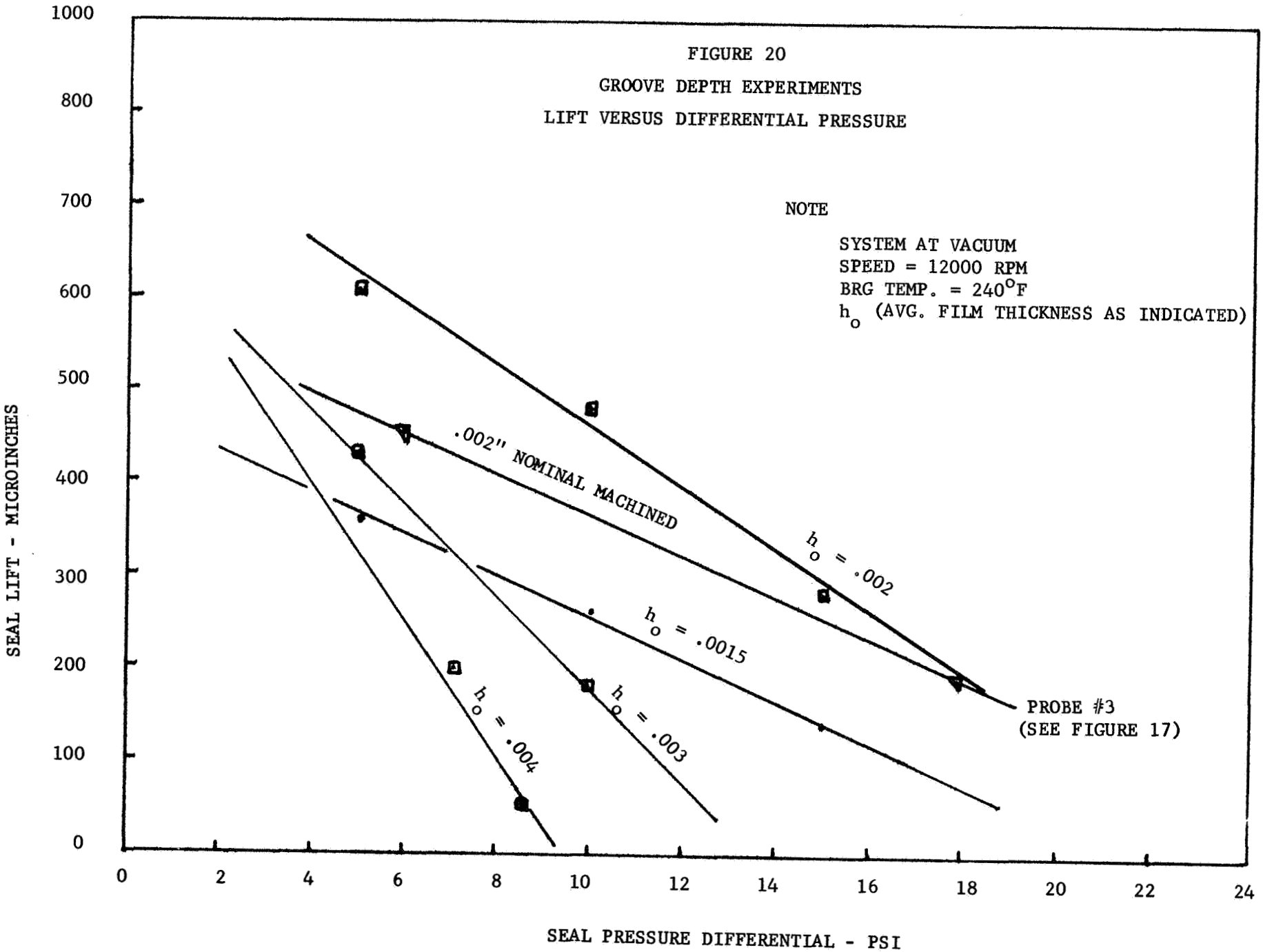
FIGURE 20
GROOVE DEPTH EXPERIMENTS
LIFT VERSUS DIFFERENTIAL PRESSURE
NOTE
SYSTEM AT VACUUM
SPEED = 12000 RPM
BRG TEMP. = 240°F
h_o (AVG. FILM THICKNESS AS INDICATED)
.002" NOMINAL MACHINED
h_o = .002
h_o = .0015
h_o = .003
h_o = .004
PROBE #3
(SEE FIGURE 17)
SEAL LIFT - MICROINCHES
SEAL PRESSURE DIFFERENTIAL - PSI
1000
800
700
600
500
400
300
200
100
0
0
2
4
6
8
10
12
14
16
18
20
22
24

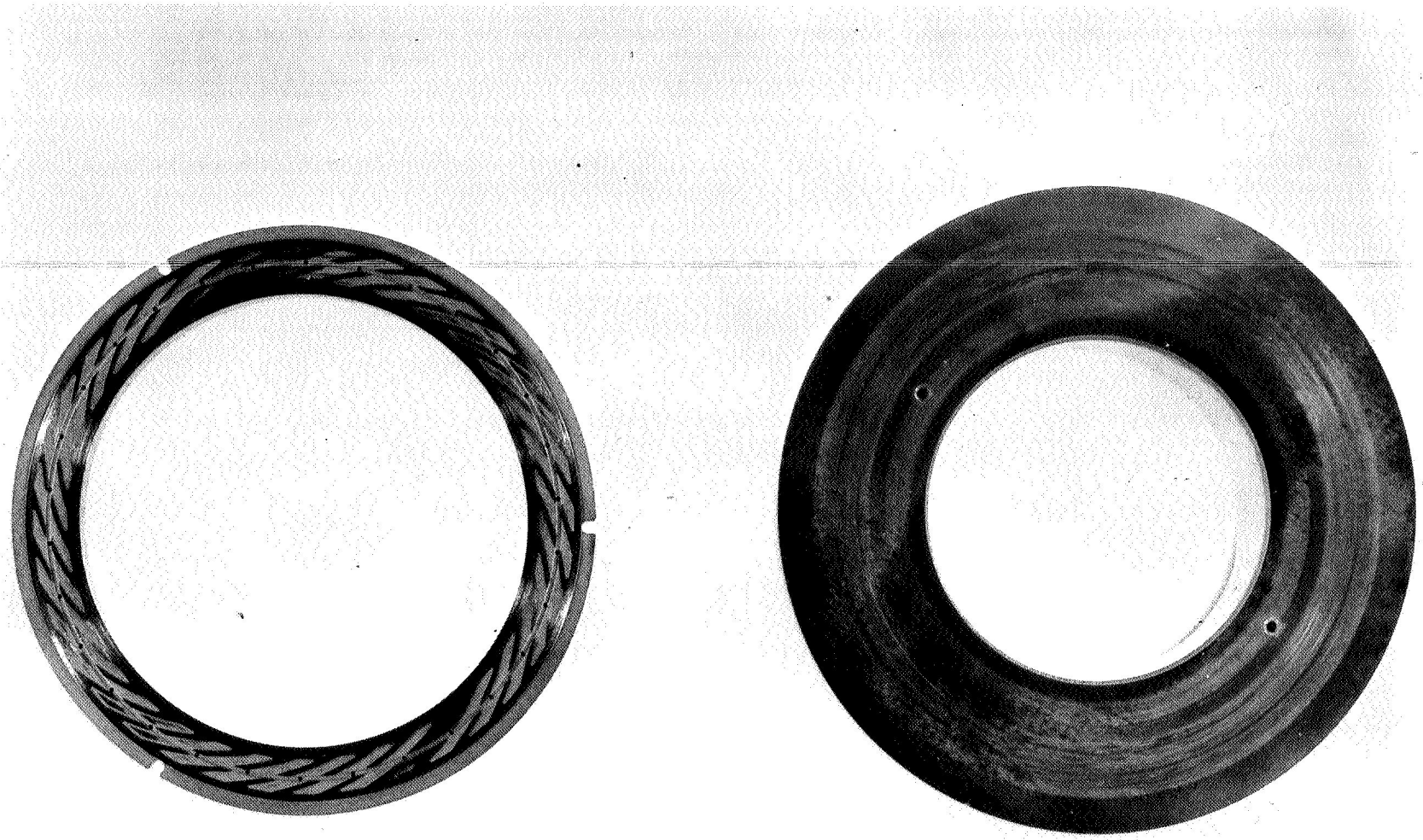

Figure 21 Steel Seal and Slinger Showing Damage

REPORT DISTRIBUTION LIST
FOR CONTRACT NO. NAS 3-11824

National Aeronautics and Space Administration (5)
Washington, D. C. 20546
Attention: P. R. Miller (RNP)
James J. Lynch (RNP)
George C. Deutsch (RR)
Dr. Fred Schulman (RNP)
H. Rochen (RNP)

National Aeronautics and Space Administration (2)
Scientific and Technical Information Facility
P. O. Box 33
College Park, Maryland 20740
Attention: Acquisitions Branch
(SQT - 34054)

National Aeronautics and Space Administration (1)
Ames Research Center
Moffett Field, California 94035
Attention: Librarian

National Aeronautics and Space Administration (1)
Goddard Space Flight Center
Greenbelt, Maryland 20771
Attention: Librarian

National Aeronautics and Space Administration (1)
Langley Research Center
Hampton, Virginia 23365
Attention: Librarian

National Aeronautics and Space Administration (1)
Manned Spacecraft Center
Houston, Texas 77001
Attention: Librarian

National Aeronautics and Space Administration (1)
George C. Marshall Space Flight Center
Huntsville, Alabama 35812
Attention: Librarian

National Aeronautics and Space Administration (1)
Jet Propulsion Laboratory
4800 Oak Grove Drive
Pasadena, California 91103
Attention: Libratian

National Aeronautics and Space Administration (14)
Lewis Research Center
21000 Brookpark Road
Cleveland, Ohio 44135
Attention: Librarian
H. O. Slone, MS 500-201
G. M. Ault, MS 3-13
P. L. Stone, MS 106-1
G. M. Thur, MS 500-202
J. E. Dilley, MS 500-309
Maxine Sabala, MS 3-19
E. R. Furman, MS 500-202
M. J. Saari, MS 500-202
Report Control Office, MS 5-5
V. F. Hlavin, MS 3-14 (Final only)
R. E. English, MS 500-201
J. Joyce, MS 500-201
E. E. Kempke, MS 500-201

National Bureau of Standards (1)
Washington, D. C. 20546
Attention: Librarian

AFSC (2)
Aeronautical Systems Division
Wright-Patterson Air Force Base, Ohio 45433
Attention: Charles Armbruster (ASRPP-10)
Librarian

AFML (1)
Wright-Patterson Air Force Base, Ohio 45433
Attention: O. O. Srp (MAMP)

Army Ordnance Frankford Arsenal (1)
Bridesburg Station
Philadelphia, Pennsylvania 19137
Attention: Librarian

U. S. Atomic Energy Commission (2)
Washington, D. C. 20545
Attention: M. J. Whitman
J.M. Simmons

Argonne National Laboratory (1)
9700 South Cass Avenue
Argonne, Illinois 60440
Attention: Librarian

Brookhaven National Laboratory (3)
Upton, Long Island, New York 11973
Attention: Librarian
Dr. D. H. Gurinsky
Dr. J. R. Weeks

Oak Ridge National Laboratory (3)
Oak Ridge, Tennessee 37831
Attention: J. Devan
R. MacPherson
Librarian

Office of Naval Research (1)
Power Division
Washington, D. C. 20360
Attention: Librarian

Bureau of Weapons (1)
Research and Engineering
Materials Division
Washington, D. C. 20546
Attention: Librarian

U. S. Naval Research Laboratory (1)
Washington, D. C. 20390
Attention: Librarian

Aerojet Nuclear Systems Company (4)
Power Systems Operations
Azusa, California 91703
Attention: J. Pope
C. Mah
A. Sellers
Librarian

AiResearch Manufacturing Company (1)
Division of the Garrett Corporation
Sky Harbor Airport
402 South 36th Street
Phoenix, Arizona 85034
Attention: Librarian

AiResearch Manufacturing Company (1)
Division of the Garrett Corporation
9851-9951 Sepulveda Boulevard
Los Angeles, California 90009
Attention: Librarian

IIT Research Institute (1)
10 West 35th Street
Chicago, Illinois 60616
Attention: Librarian

North American Aviation, Inc. (1)
Atomics International Division
8900 DeSoto Avenue
Canoga Park, California 91304
Attention: Librarian

AVCO (1)
Research & Advanced Development Department
201 Lowell Street
Wilmington, Massachusetts 01887
Attention: Librarian

Electro-Optical Systems, Inc. (1)
Advanced Power Systems Division
Pasadena, California 91107
Attention: Librarian

Philco Corporation (1)
Aeronutronics
Newport Beach, California 92663
Attention: Librarian

General Dynamics Corporation (1)
General Atomic Division
John Jay Hopkins Lab
P. O. Box 608
San Diego, California 92112
Attention: Librarian

General Electric Company (1)
Nuclear Systems Programs
Missile & Space Division
Cincinnati, Ohio 45215
Attention: R. D. Brooks

General Electric Company (1)
Missile and Space Vehicle Department
3198 Chestnut Street
Philadelphia, Pennsylvania 19104
Attention: Librarian

General Dynamics/Fort Worth (1)
P. O. Box 748
Fort Worth, Texas 76101
Attention: Librarian

General Motors Corporation (1)
Allison Division
Indianapolis, Indiana 46206
Attention: Librarian

Hamilton Standard (1)
Division of United Aircraft Corporation
Windsor Locks, Connecticut 06096
Attention: Librarian

Hughes Aircraft Company (1)
Engineering Division
Culver City, California 90230
Attention: Librarian

Lawrence Radiation Laboratory (1)
Livermore, California 94550
Attention: Librarian

Lockheed Missiles and Space Division (1)
Lockheed Aircraft Corporation
Sunnyvale, California 90221
Attention: Librarian

Teledyne Isotopes (1)
Nuclear Systems Division
110 West Temonium Road
Temonium, Maryland 21093

Martin Marietta Corporation (1)
Metals Technology Laboratory
Wheeling, Illinois 60090

Materials Research Corporation (1)
Orangeburg, New York 10962
Attention: Librarian

McDonnell Aircraft (1)
St. Louis, Missouri 63166
Attention: Librarian

MSA Research Corporation (1)
Callery, Pennsylvania 16024
Attention: Librarian

National Research Corporation
70 Memorial Drive
Cambridge, Massachusetts 02142
Attention: Librarian

North American Aviation (1)
Los Angeles Division
Los Angeles, California 90009
Attention: Librarian

United Aircraft Corporation (1)
Pratt & Whitney Aircraft Division
400 Main Street
East Hartford, Connecticut 06108
Attention: Librarian

Republic Aviation Corporation (1)
Farmingdale, Long Island, New York 11735
Attention: Librarian

Sandia Corporation (1)
P. O. Box 5800
Albuquerque, New Mexico 87116
Attention: Librarian

Solar (1)
2200 Pacific Highway
San Diego, California 92112
Attention: Librarian

Southwest Research Institute (1)
8500 Culebra Road
San Antonio, Texas 78228
Attention: Librarian

Superior Tube Company (1)
Norristown, Pennsylvania 19404
Attention: Librarian

TRW Inc. (1)
23555 Euclid Avenue
Cleveland, Ohio 44117
Attention: Librarian

Union Carbide Corporation (2)
1020 West Park Avenue
Kokomo, Indiana 46901
Attention: Librarian
Technology Department

Westinghouse Electric Corporation (1)
Astronuclear Laboratory
P. O. Box 10864
Pittsburgh, Pennsylvania 15236
Attention: Librarian

Wah Chang Corporation (1)
Albany, Oregon 97321
Attention: Librarian

Whittaker Corporation (1)
Nuclear Metals Division
West Concord, Massachusetts 01781
Attention: Librarian

Wright-Patterson Air Force Base (1)
Research and Technology Division
Dayton, Ohio 45404
Attention: M. P. Wannemacher, APIP-1

Defense Metals Information Center (2)
Battelle Memorial Institute
Columbus Laboratories
505 King Avenue
Columbus, Ohio 43201
Attention: R. T. Niehoff
Librarian

Mechanical Technology, Inc. (1)
Latham, New York 12110
Attention: Librarian